

NASA TECHNICAL NOTE



NASA TN D-3791

C.1

LOAN COPY: RETURN TO
AFWL (WLIL-2)
KIRTLAND AFB, N MEX.



NASA TN D-3791

VIBRATION ANALYSIS OF
CYLINDRICALLY CURVED PANELS WITH
SIMPLY SUPPORTED OR CLAMPED EDGES
AND COMPARISON WITH SOME EXPERIMENTS

by John L. Sewall

Langley Research Center

Langley Station, Hampton, Va.





0130509

NASA TN D-3791

VIBRATION ANALYSIS OF CYLINDRICALLY CURVED PANELS
WITH SIMPLY SUPPORTED OR CLAMPED EDGES AND
COMPARISON WITH SOME EXPERIMENTS

By John L. Sewall

Langley Research Center
Langley Station, Hampton, Va.

NATIONAL AERONAUTICS AND SPACE ADMINISTRATION

For sale by the Clearinghouse for Federal Scientific and Technical Information
Springfield, Virginia 22151 – Price \$2.00

VIBRATION ANALYSIS OF CYLINDRICALLY CURVED PANELS
WITH SIMPLY SUPPORTED OR CLAMPED EDGES AND
COMPARISON WITH SOME EXPERIMENTS

By John L. Sewall
Langley Research Center

SUMMARY

The natural frequencies of cylindrically curved panels are calculated by application of the classical energy method employing the Rayleigh-Ritz procedure and are compared with measured frequencies of rectangular and square panels fastened at their edges by means of closely spaced bolts. The mode shapes used in the calculations are products of functions based on beam vibration mode shapes and satisfying geometrical edge conditions in both longitudinal and circumferential directions.

General frequency equations are derived, and their applications to panels of small curvature lead to simplified Rayleigh-type frequency equations which were more satisfactory for certain modal combinations and edge conditions than for others. Measured frequencies were, for the most part, bracketed by calculated frequencies based on simply supported or fully clamped edges and, at low-order circumferential modes, were generally closer to calculated frequencies for simply supported edges but showed some tendency to move closer to calculated frequencies for clamped edges as the circumferential mode number increased. This behavior is attributed partly to membrane effects due to panel curvature and partly to complicated edge conditions due to the use of simple lap attachments which could not be represented adequately by theory. Comparison of experimental frequencies with inextensional frequencies, calculated with longitudinal and/or circumferential membrane strains omitted, indicated that actual panel mountings may have provided greater edge fixity along curved rather than along straight edges.

Further efforts to bring experimental and theoretical frequencies into closer agreement should include vibration tests on curved panels with edges designed to simulate simply supported or clamped conditions as closely as possible. In addition, the effects of modal functions other than beam functions should be examined, and other methods of analysis, such as those involving finite difference or finite element techniques, should be applied.

INTRODUCTION

Knowledge of the vibration characteristics of curved panels is important to designers confronted with aeroelastic and acoustic problems in aerospace vehicle structures in which curved panels are important structural components. Curved panels, like flat panels, possess many vibration modes which can respond to such dynamic forces as those due to acoustic excitation and unsteady aerodynamic flow. Panel frequencies and mode shapes can be greatly affected by both curvature and edge support conditions. This paper is concerned with both of these effects in comparisons of analytical and experimental frequencies of some thin curved panels.

Previous studies applicable to the vibrations of cylindrically curved panels are reported in references 1 to 6 for various combinations of edge conditions. In reference 1, Reissner derives frequency equations for thin paraboloidal shallow shell elements with simply supported rectangular boundaries. Palmer (ref. 2) gives frequency equations for both simply supported and clamped-edge rectangular and square panels curved in both directions, but these equations are restricted to the mode with one half-wave in each direction. Forsberg's work, involving the direct numerical solution of the differential equations of motion of cylindrical shells (ref. 3), is applicable to cylindrically curved panels with simply supported straight edges and simply supported, clamped, or free curved edges, and various combinations of these. In an extensive analytical treatment of the dynamic behavior of thin shallow shells of double curvature, Oniashvili in reference 4, following an approach advocated by Vlasov in reference 5, considers the more general case of arbitrary support conditions, with the mode shapes in each direction approximated by beam vibration functions. Some results are included in reference 4 showing the effects of curvature and edge clamping on the natural frequencies of spherically curved panels, but most of the other examples, together with some experimental results on particular shell-roof configurations, are concerned with shell elements having simply supported edges. Very little, if any, correlation between theory and experiment is to be found in these references. However, in a very recent paper (ref. 6) an extensive series of vibration experiments on cylindrically curved panels is reported as part of a larger investigation concerned with sonic fatigue, and comparisons are made with the results of a vibration analysis based on a modal approach employing beam modes, as in reference 4.

The present paper is exclusively concerned with the vibration of panels of small curvature, and its purpose is to report a study of the effects of curvature and edge conditions on the natural frequencies of some cylindrically curved panels for which experimental frequency and mode shape data are known. The experimental data of reference 6 are used, together with the data of references 7 and 8, for panels of various radii of curvature, including the limiting case of infinite radius (that is, flat panel). The panels of

references 6 and 7 are rectangular and have very nearly the same dimensions but different thicknesses. The panels of reference 8 are square, and the frequencies apply to just one panel thickness (namely, 0.020 in. (0.051 cm)). Experimental frequencies obtained in the same series of tests as reference 8 for other thicknesses (0.032 in. (0.081 cm) and 0.040 in. (0.10 cm)), but not heretofore published, are included in the present paper and compared with calculated frequencies.

Calculated frequencies in the present paper were obtained by a straightforward application of the classical energy method employing the Rayleigh-Ritz procedure from which general frequency equations for arbitrary edge conditions are derived in the same manner as in references 9 and 10 for the vibrations of flat panels. Shell membrane and bending effects are both included. Applications are based on the use of elementary beam vibration functions to approximate the mode shapes of the panel, as is done in references 4 to 6. Simplifications involving modal decoupling of the general Rayleigh-Ritz equations due to the use of beam functions are shown to lead to a general approximate expression that is applicable to several different combinations of edge conditions.

The main body of the paper begins with the development of the general frequency equations followed by applications involving the use of beam functions and leading to a general approximate frequency equation and also to particular frequency equations for clamped-edge and simply supported curved panels. Although the main emphasis is on curvature and edge conditions, the effects of panel thickness are also discussed.

SYMBOLS

a	radius of curvature to middle surface of panel (see fig. 1)
$\left. \begin{array}{l} a_{mn}(t) \\ b_{mn}(t) \\ c_{mn}(t) \end{array} \right\}$	amplitude functions in assumed modal expansions (see eqs. (5) and (6))
$\left. \begin{array}{l} A_{pq} \\ B_{pq} \\ E_{pq} \\ F_{pq} \\ G_{pq} \end{array} \right\}$	matrix elements in Rayleigh-Ritz frequency equations

$\left. \begin{array}{l} H_{pq} \\ J_{pq} \\ K_{pq} \\ M_{pq} \end{array} \right\}$	matrix elements in Rayleigh-Ritz frequency equations
C	extensional (or membrane) stiffness, $\frac{Eh}{1 - \mu^2}$
D	bending stiffness, $\frac{Eh^3}{12(1 - \mu^2)}$
E	Young's modulus
h	panel thickness
I_1 to I_6	surface integrals involving modal functions
l	length of panel along straight edges (see fig. 1)
m	integer denoting longitudinal modal component (number of axial half-waves for a panel with simply supported curved edges)
n	integer denoting circumferential modal component (number of circumferential half-waves for a panel with simply supported straight edges)
$N_{m,n}$	eigenvalue of beam-mode approximation
s	circumferential coordinate (see fig. 1)
t	time
T	kinetic energy
U	strain energy
u,v,w	displacements of panel (see fig. 1)

x	longitudinal coordinate (see fig. 1)
$X_m(x)$	longitudinal mode shape component
$Y_n(s)$	circumferential mode shape component
α	central angle of panel (see fig. 1)
$\beta_{m,n} = N_m l$ or $N_n \alpha a$	
Δ	eigenvalue of frequency equation, $\frac{\rho h \omega^2}{C}$
$\bar{\Delta}$	dimensionless eigenvalue, $\frac{l \alpha a}{\pi^2 h} \sqrt{\Delta}$
$\epsilon_1, \epsilon_2, \epsilon_3$	membrane strains (see, for example, eqs. (2))
$\gamma_{m,n}$	coefficient in beam mode approximation
$\kappa_1, \kappa_2, \kappa_{12}$	changes of curvature (see, for example, eqs. (2))
μ	Poisson's ratio
ρ	mass density of panel
ω	angular frequency, radians per second
$X'_m(x) = \frac{d}{dx} X_m(x); \quad X''_m(x) = \frac{d^2}{dx^2} X_m(x)$	
$Y'_n(s) = \frac{d}{ds} Y_n(s); \quad Y''_n(s) = \frac{d^2}{ds^2} Y_n(s)$	
Subscripts:	
E	extensional
j,m	longitudinal modal integers
I	inextensional
k,n	circumferential modal integers

p,q	general modal integers
x	denotes differentiation with respect to x
s	denotes differentiation with respect to s

Dots over quantities denote differentiation with respect to time.

METHOD OF ANALYSIS

The method of analysis used in this paper is the classical energy method employing the Rayleigh-Ritz procedure in which the longitudinal, circumferential, and radial (or normal) displacements u , v , and w indicated in figure 1 are each represented in terms of an arbitrary number of products of longitudinal and circumferential mode shapes. Two general frequency equations are derived, one in which the strain energy is written in terms of the complete strain-displacement relations given by Sanders in reference 11, and the other in which the simplifying relations of Donnell (ref. 12) are employed. These equations are given in terms of general longitudinal and circumferential mode-shape components. In the application of the method of analysis, functions for these components are chosen to satisfy desired edge conditions, and in the present paper the choice of beam vibration functions leads to a simplified frequency equation for curved panels with various combinations of edge conditions. Particular forms of this equation are also included for curved panels with all edges fully clamped and with all edges simply supported.

Derivation of General Frequency Equations

The essential steps in the derivation are the same for both general frequency equations and are presented for the equation based on the complete strain-displacement relations of reference 11 with in-plane inertias retained.

Strain energy and strain-displacement relations. - The strain energy for a thin isotropic cylindrically curved panel of thickness h may be written as

$$\begin{aligned}
 U = & \frac{C}{2} \int_0^{\alpha a} \int_0^l \left(\epsilon_1^2 + 2\mu \epsilon_1 \epsilon_2 + \epsilon_2^2 + \frac{1-\mu}{2} \epsilon_{12}^2 \right) dx ds \\
 & + \frac{D}{2} \int_0^{\alpha a} \int_0^l \left[\kappa_1^2 + 2\mu \kappa_1 \kappa_2 + \kappa_2^2 + 2(1-\mu) \kappa_{12}^2 \right] dx ds
 \end{aligned} \tag{1}$$

where l is the length along the straight edges, αa the length along the curved edges as shown in figure 1, C is the extensional (or membrane) stiffness $\frac{Eh}{1 - \mu^2}$, and D is the inextensional (or bending) stiffness $\frac{Eh^3}{12(1 - \mu^2)}$, E being Young's modulus and μ Poisson's ratio.

The quantities $\epsilon_1, \epsilon_2, \dots, \kappa_{12}$ in equation (1) are strains and changes of curvature which may be written in terms of Sanders' displacement functions in reference 11:

$$\left. \begin{aligned} \epsilon_1 &= u_x \\ \epsilon_2 &= v_s + \frac{w}{a} \\ \epsilon_{12} &= v_x + u_s \\ \kappa_1 &= -w_{xx} \\ \kappa_2 &= -w_{ss} + \frac{v_s}{a} \\ \kappa_{12} &= -w_{xs} + \frac{3v_x}{4a} - \frac{u_s}{4a} \end{aligned} \right\} \quad (2)$$

where

ϵ_1	longitudinal membrane strain
ϵ_2	circumferential membrane strain
ϵ_{12}	middle surface shear strain
κ_1	longitudinal change of curvature
κ_2	circumferential change of curvature
κ_{12}	torsional change of curvature

Subscripts on the displacements denote differentiation with respect to x and/or s .

The strain-displacement relations due to Donnell (ref. 12) are the same as equations (2) except for the neglect of circumferential and longitudinal contributions to the changes of curvature; thus κ_2 and κ_{12} are reduced to

$$\left. \begin{aligned} \kappa_2 &\approx -w_{ss} \\ \kappa_{12} &\approx -w_{xs} \end{aligned} \right\} \quad (3)$$

Kinetic energy.- The total kinetic energy may be written as

$$T = \frac{\rho h}{2} \int_0^{\alpha a} \int_0^l (\dot{u}^2 + \dot{v}^2 + \dot{w}^2) dx ds \quad (4)$$

where ρ is the mass density of the panel and where dots over the displacements denote differentiation with respect to time.

Modal functions.- The displacements u , v , and w are assumed to be of the form

$$\left. \begin{aligned} u(x,s,t) &= \sum_m \sum_n a_{mn}(t) X'_m(x) Y_n(s) \\ v(x,s,t) &= \sum_m \sum_n b_{mn}(t) X_m(x) Y'_n(s) \\ w(x,s,t) &= \sum_m \sum_n c_{mn}(t) X_m(x) Y_n(s) \end{aligned} \right\} \quad (5)$$

where $a_{mn}(t)$, $b_{mn}(t)$, and $c_{mn}(t)$ are time-dependent amplitude functions and m and n are integers identifying the longitudinal and circumferential mode shape components X_m and Y_n , which are chosen to satisfy desired edge conditions. Primes on X_m and Y_n denote $\frac{d}{dx} X_m$ and $\frac{d}{ds} Y_n$, respectively.

General equations of motion and frequency equation.- With the use of equations (2) in equation (1), the strain energy becomes a function of u , v , and w and their spatial derivatives. Next, both strain and kinetic energies are obtained in terms of the modal functions in equations (5). With the assumption of simple harmonic motion of frequency ω

$$\left. \begin{aligned} a_{mn}(t) &= \bar{a}_{mn} e^{i\omega t} \\ b_{mn}(t) &= \bar{b}_{mn} e^{i\omega t} \\ c_{mn}(t) &= \bar{c}_{mn} e^{i\omega t} \end{aligned} \right\} \quad (6)$$

the total energy of the system is minimized with respect to the amplitudes \bar{a}_{mn} , \bar{b}_{mn} , and \bar{c}_{mn} in accordance with the Rayleigh-Ritz procedure to obtain the equations of motion. The basic relations involved in this minimization for the j th longitudinal and k th circumferential modal combination may be written as

$$\left. \begin{aligned} \frac{\partial}{\partial \bar{a}_{jk}} [U(x,s) - \omega^2 T(x,s)] &= 0 \\ \frac{\partial}{\partial \bar{b}_{jk}} [U(x,s) - \omega^2 T(x,s)] &= 0 \\ \frac{\partial}{\partial \bar{c}_{jk}} [U(x,s) - \omega^2 T(x,s)] &= 0 \end{aligned} \right\} \quad (7)$$

where $U(x,s)$ and $T(x,s)$ are the maximum strain and kinetic energies written in terms of equations (2), (5), and (6). By carrying out the operations indicated in equations (7) for an arbitrary number of modal products approximating each of the displacements u , v , and w , a general set of equations of motion is obtained and may be put in matrix form as follows:

$$\begin{bmatrix} [A] & -\Delta[B] & \vdots & [E] & \vdots & [G] \\ & [E]' & [F] & -\Delta[H] & \vdots & [J] \\ & [G]' & \vdots & [J]' & [K] & -\Delta[M] \end{bmatrix} \begin{Bmatrix} \{\bar{a}\} \\ \{\bar{b}\} \\ \{\bar{c}\} \end{Bmatrix} = 0 \quad (8)$$

where each submatrix represents a dual row and column identification due to the double summations in the derivations of the equations. For example, $[A]$ is equivalent

to $\sum_j \sum_k \sum_n^{\rightarrow} [A]$ and $\{\bar{a}\}$ to $\left\{ \sum_j \sum_k \sum_n^{\rightarrow} \bar{a} \right\}^m$. Primes on matrices denote transposed matrices.

The condition that equation (8) have nontrivial solutions is that the determinant of the amplitude matrices $\{\bar{a}\}$, $\{\bar{b}\}$, and $\{\bar{c}\}$ vanish. This condition gives the general frequency equation

$$\begin{vmatrix} [A] & -\Delta[B] & \vdots & [E] & \vdots & [G] \\ & [E]' & [F] & -\Delta[H] & \vdots & [J] \\ & [G]' & \vdots & [J]' & [K] & -\Delta[M] \end{vmatrix} = 0 \quad (9)$$

where Δ is a dimensional eigenvalue or frequency parameter given by

$$\Delta = \frac{\rho h \omega^2}{C}$$

and where

$$A_{pq} = \int_0^{\alpha a} \int_0^l X_j'' X_m'' Y_k Y_n dx ds + \frac{1-\mu}{2} \left(1 + \frac{D}{4a^2 C} \right) \int_0^{\alpha a} \int_0^l X_j' X_m' Y_k' Y_n' dx ds$$

$$B_{pq} = \int_0^{\alpha a} \int_0^l X_j' X_m' Y_k Y_n dx ds$$

$$E_{pq} = \mu \int_0^{\alpha a} \int_0^l X_j'' X_m Y_k Y_n'' dx ds + \frac{1-\mu}{2} \left(1 - \frac{3D}{4a^2 C} \right) \int_0^{\alpha a} \int_0^l X_j' X_m' Y_k' Y_n' dx ds$$

$$G_{pq} = \frac{1}{a} \left[\mu \int_0^{\alpha a} \int_0^l X_j'' X_m Y_k Y_n dx ds + \frac{1-\mu}{2} \left(\frac{D}{C} \right) \int_0^{\alpha a} \int_0^l X_j' X_m' Y_k' Y_n' dx ds \right]$$

$$F_{pq} = \left(1 + \frac{D}{a^2 C} \right) \int_0^{\alpha a} \int_0^l X_j X_m Y_k'' Y_n'' dx ds + \frac{1-\mu}{2} \left(1 + \frac{9D}{4a^2 C} \right) \int_0^{\alpha a} \int_0^l X_j' X_m' Y_k' Y_n' dx ds$$

$$H_{pq} = \int_0^{\alpha a} \int_0^l X_j X_m Y_k' Y_n' dx ds$$

$$J_{pq} = \frac{1}{a} \left\{ \int_0^{\alpha a} \int_0^l X_j X_m Y_k'' Y_n dx ds - \frac{D}{C} \left[\mu \int_0^{\alpha a} \int_0^l X_j X_m'' Y_k'' Y_n dx ds \right. \right. \\ \left. \left. + \int_0^{\alpha a} \int_0^l X_j X_m Y_k'' Y_n'' dx ds + \frac{3(1-\mu)}{2} \int_0^{\alpha a} \int_0^l X_j' X_m' Y_k' Y_n' dx ds \right] \right\}$$

$$K_{pq} = \frac{1}{a^2} \int_0^{\alpha a} \int_0^l X_j X_m Y_k Y_n dx ds + \frac{D}{C} \left[\int_0^{\alpha a} \int_0^l X_j'' X_m'' Y_k Y_n dx ds \right. \\ \left. + \mu \int_0^{\alpha a} \int_0^l (X_j X_m'' Y_k'' Y_n + X_j'' X_m Y_k Y_n'') dx ds + \int_0^{\alpha a} \int_0^l X_j X_m Y_k'' Y_n'' dx ds \right. \\ \left. + 2(1-\mu) \int_0^{\alpha a} \int_0^l X_j' X_m' Y_k' Y_n' dx ds \right]$$

$$M_{pq} = \int_0^{\alpha a} \int_0^l X_j X_m Y_k Y_n dx ds$$

The matrices $[A]$, $[B]$, $[F]$, $[H]$, $[K]$, and $[M]$ are all symmetric with respect to their individual diagonals, and the other matrices are symmetric with respect to the main diagonal through the relations $E'_{qp} = E_{pq}$, $G'_{qp} = G_{pq}$, and $J'_{qp} = J_{pq}$. The subscripts p and q identify a particular location in the overall matrix of equation (9) and are associated with j,m and k,n , respectively.

Once the eigenvalues are obtained from equation (9), the corresponding eigenvectors are determined from equation (8) in the form of amplitude ratios, and the mode shapes of the curved panel are in turn obtained from equations (5) which, for this purpose, may be written in the form

$$\left. \begin{aligned} \bar{u}(x,s) &= \sum_m \sum_n \frac{\bar{a}_{mn}}{\bar{c}_{jk}} X'_m(x) Y_n(s) \\ \bar{v}(x,s) &= \sum_m \sum_n \frac{\bar{b}_{mn}}{\bar{c}_{jk}} X_m(x) Y'_n(s) \\ \bar{w}(x,s) &= \sum_m \sum_n \frac{\bar{c}_{mn}}{\bar{c}_{jk}} X_m(x) Y_n(s) \end{aligned} \right\} \quad (10)$$

where \bar{u} , \bar{v} , and \bar{w} are nondimensional displacements and $\frac{\bar{a}_{mn}}{\bar{c}_{jk}}$, $\frac{\bar{b}_{mn}}{\bar{c}_{jk}}$, and $\frac{\bar{c}_{mn}}{\bar{c}_{jk}}$

are the corresponding amplitude ratios arbitrarily referred to the j,k th amplitude coefficient in the w -approximation.

General shallow-shell frequency equation.- With the use of the Donnell strain-displacement relations (eqs. (3) and the first four strain-displacement relations in eqs. (2)), an approximate frequency equation may be derived in the same manner as equation (9). If, in addition, the in-plane velocity terms \dot{u} and \dot{v} are omitted from the kinetic energy (eq. (4)), the following frequency equation is obtained:

$$\begin{vmatrix} [A] & [E] & & [G] \\ [E]' & [F] & & [J] \\ [G]' & [J]' & [K] & -\Delta[M] \end{vmatrix} = 0 \quad (11)$$

where

$$A_{pq} = \int_0^{\alpha a} \int_0^l X_j'' X_m'' Y_k Y_n dx ds + \frac{1-\mu}{2} \int_0^{\alpha a} \int_0^l X_j' X_m' Y_k' Y_n' dx ds$$

$$E_{pq} = \mu \int_0^{\alpha a} \int_0^l X_j'' X_m Y_k Y_n'' dx ds + \frac{1-\mu}{2} \int_0^{\alpha a} \int_0^l X_j' X_m' Y_k' Y_n' dx ds$$

$$G_{pq} = \frac{\mu}{a} \int_0^{\alpha a} \int_0^l X_j'' X_m Y_k Y_n dx ds$$

$$F_{pq} = \int_0^{\alpha a} \int_0^l X_j X_m Y_k'' Y_n'' dx ds + \frac{1-\mu}{2} \int_0^{\alpha a} \int_0^l X_j' X_m' Y_k' Y_n' dx ds$$

$$J_{pq} = \frac{1}{a} \int_0^{\alpha a} \int_0^l X_j X_m Y_k'' Y_n dx ds$$

and where K_{pq} , M_{pq} , and Δ are the same as in equation (9). The mode shapes can be determined from equations (10) as before.

Equation (11) may be considered to be satisfactory for calculating the frequencies of curved panels as long as the panel curvature $\frac{1}{a}$ is not too large. A measure of the actual limit of curvature is provided by a shallow-shell criterion given in reference 5 (p. 343), for example, in which a shell element is considered to be shallow, or a plate slightly curved, if the rise (see fig. 1) is not more than one-fifth the smallest side of the plate lying in the plane of its supports. Berry and Reissner in reference 13 suggest a value of one-eighth for this ratio but indicate that it could be higher.

Reduction to a flat panel.— For the limiting case of a flat panel, the curvature reduces to zero so that the G- and J-matrices vanish, and thereby leave the membrane and bending contributions to the frequency completely uncoupled from one another. The general frequency equation in bending of a flat panel, obtained from equations (9) or (11) when $\frac{1}{a} = 0$, may be written as

$$\left| \begin{bmatrix} K^{(B)} \end{bmatrix} - \frac{\rho h \omega^2}{D} \begin{bmatrix} M \end{bmatrix} \right| = 0 \quad (12)$$

where

$$\begin{aligned}
K_{pq}^{(B)} = & \int_0^{\alpha a} \int_0^l X_j'' X_m'' Y_k Y_n \, dx \, ds + \int_0^{\alpha a} \int_0^l X_j X_m Y_k'' Y_n'' \, dx \, ds \\
& + \mu \int_0^{\alpha a} \int_0^l (X_j X_m'' Y_k'' Y_n + X_j'' X_m Y_k Y_n'') \, dx \, ds \\
& + 2(1 - \mu) \int_0^{\alpha a} \int_0^l X_j' X_m' Y_k' Y_n' \, dx \, ds
\end{aligned}$$

and the elements of the M-matrix are unchanged from those in equation (9). Equation (12) is essentially the same equation as that given by Young in reference 9.

Certain inextensional considerations.- The frequency equation for inextensional (or bending) vibrations of a cylindrically curved panel may also be obtained by omitting the circumferential strain ϵ_2 in the derivation of equations (9) and (11). By simply setting ϵ_2 equal to zero, the extensional (or membrane) terms are eliminated from the elements of the G- and J-matrices, which reduce to zero in the case of equation (11); thus, extensional and inextensional contributions to the frequency uncouple and lead to equation (12) as before. When the longitudinal strain ϵ_1 is set equal to zero, extensional terms are eliminated only from the elements of the G-matrices, and an inextensional frequency equation cannot, in general, be obtained unless ϵ_2 is also zero or unless the straight edges are unrestrained against circumferential displacement v . Further consideration of these effects is given later in the comparisons of theory and experiment for particular edge conditions.

Applications of Method of Analysis

Although the choice of functions for the X- and Y-components in equations (5) is, of course, arbitrary, the functions of a vibrating uniform beam are particularly attractive choices because they lead, by virtue of orthogonality properties, to significant simplifications in the frequency equation. These functions have been employed previously in the vibration analysis of flat panels (for example, refs. 9 and 10) and are assumed in the present analysis to be satisfactory for curved panels as long as the panel curvature is small. Because of this limitation on panel curvature, it is both sufficient and consistent to confine the application of beam vibration functions to the shallow-shell frequency equation (eq. (11)) for which upper limits to the panel curvature have already been suggested. Thus, the applications to follow are demonstrated with the beam functions used in equation (11), although these functions could be used in equation (9) as well, as is discussed later.

Simplifications due to the use of beam functions.- With the X- and Y-components approximated by means of beam vibration functions, the following orthogonality properties hold for any two opposite edges ideally clamped, simply supported, or free:

$$\left. \begin{aligned}
 & \left. \begin{aligned}
 \int_0^l X_j X_m dx &= \int_0^l X_m^2 dx \\
 \int_0^l X_j'' X_m'' dx &= \int_0^l (X_m'')^2 dx
 \end{aligned} \right\} & (j = m) \\
 & \left. \begin{aligned}
 \int_0^{\alpha a} Y_k Y_n ds &= \int_0^{\alpha a} Y_n^2 ds \\
 \int_0^{\alpha a} Y_k'' Y_n'' ds &= \int_0^{\alpha a} (Y_n'')^2 ds
 \end{aligned} \right\} & (k = n) \\
 & \int_0^l X_j X_m dx = \int_0^l X_j'' X_m'' dx = 0 & (j \neq m) \\
 & \int_0^{\alpha a} Y_k Y_n ds = \int_0^{\alpha a} Y_k'' Y_n'' ds = 0 & (k \neq n)
 \end{aligned} \right\} \quad (13)$$

As a consequence of these relations, the elements of equation (11) may be simplified as follows:

$$\left. \begin{aligned}
 A_{pq} = A_{mn} &= \int_0^{\alpha a} \int_0^l (X_m'' Y_n)^2 dx ds + \frac{1-\mu}{2} \int_0^{\alpha a} \int_0^l (X_m' Y_n')^2 dx ds & (j = m; k = n) \\
 A_{pq} &= \frac{1-\mu}{2} \int_0^{\alpha a} \int_0^l X_j' X_m' Y_k' Y_n' dx ds & (j \neq m \text{ and/or } k \neq n) \\
 E_{pq} = E_{mn} &= \mu \int_0^{\alpha a} \int_0^l X_m'' X_m Y_n'' Y_n dx ds \\
 &+ \frac{1-\mu}{2} \int_0^{\alpha a} \int_0^l (X_m' Y_n')^2 dx ds & (j = m; k = n)
 \end{aligned} \right\}$$

(Equation continued on next page)

$$\begin{aligned}
E_{pq} &= \mu \int_0^{\alpha a} \int_0^l X_j'' X_m Y_k Y_n'' dx ds + \frac{1-\mu}{2} \int_0^{\alpha a} \int_0^l X_j' X_m' Y_k' Y_n' dx ds & (j \neq m; k \neq n) \\
G_{pq} &= G_{mn} = \frac{\mu}{a} \int_0^{\alpha a} \int_0^l X_m'' X_m Y_n^2 dx ds & (j = m; k = n) \\
G_{pq} &= G_{jm} = \frac{\mu}{a} \int_0^{\alpha a} \int_0^l X_j'' X_m Y_n^2 dx ds & (j \neq m; k = n) \\
G_{pq} &= 0 & (k \neq n) \\
F_{pq} &= F_{mn} = \int_0^{\alpha a} \int_0^l (X_m Y_n'')^2 dx ds + \frac{1-\mu}{2} \int_0^{\alpha a} \int_0^l (X_m' Y_n')^2 dx ds & (j = m; k = n) \\
F_{pq} &= A_{pq} & (j \neq m \text{ and/or } k \neq n) \\
J_{pq} &= J_{mn} = \frac{1}{a} \int_0^{\alpha a} \int_0^l X_m^2 Y_n'' Y_n dx ds & (j = m; k = n) \\
J_{pq} &= J_{kn} = \frac{1}{a} \int_0^{\alpha a} \int_0^l X_m^2 Y_k'' Y_n dx ds & (j = m; k \neq n) \\
J_{pq} &= 0 & (j \neq m) \\
K_{pq} &= K_{mn} = \frac{1}{a^2} \int_0^{\alpha a} \int_0^l (X_m Y_n)^2 dx ds + \frac{D}{C} \left[\int_0^{\alpha a} \int_0^l (X_m'' Y_n)^2 dx ds \right. \\
&\quad + 2\mu \int_0^{\alpha a} \int_0^l (X_m X_m'' Y_n Y_n'') dx ds + \int_0^{\alpha a} \int_0^l (X_m Y_n'')^2 dx ds \\
&\quad \left. + 2(1-\mu) \int_0^{\alpha a} \int_0^l (X_m' Y_n')^2 dx ds \right] & (j = m; k = n) \\
K_{pq} &= \frac{D}{C} \left[\mu \int_0^{\alpha a} \int_0^l (X_j X_m'' Y_k'' Y_n + X_j'' X_m Y_k Y_n'') dx ds \right. \\
&\quad \left. + 2(1-\mu) \int_0^{\alpha a} \int_0^l X_j' X_m' Y_k' Y_n' dx ds \right] & (j \neq m \text{ and/or } k \neq n) \\
M_{pq} &= M_{mn} = \int_0^{\alpha a} \int_0^l (X_m Y_n)^2 dx ds & (j = m; k = n) \\
M_{pq} &= 0 & (j \neq m \text{ and/or } k \neq n)
\end{aligned}$$

(14)

The integrals in equations (14) may be evaluated by use of reference 14.

Modal coupling properties for certain beam-mode combinations.- For certain modal combinations and edge conditions, the off-diagonal matrix elements vanish, and the frequency equation may be simplified still further. For example, with opposite edges simply supported and

$$\left. \begin{aligned} X_m &= \sin \frac{m\pi x}{l} \\ Y_n &= \sin \frac{n\pi s}{\alpha a} \end{aligned} \right\} \quad (15)$$

the off-diagonal integrals are zero for all modal combinations of $j \neq m$ or $k \neq n$. This statement is also true when the opposite edges are fully clamped or free (at least for the elastic free-free modes) and when $j + m$ or $k + n$ is odd, on the basis of the single-integral evaluations given in forms 16 and 20 of reference 14. For example, with the curved edges clamped, the single integrals

$$\int_0^l X'_j X'_m dx = - \int_0^l X_j X''_m dx = \frac{4N_j^2 N_m^2 (\gamma_j N_j - \gamma_m N_m)}{N_m^4 - N_j^4} \left[(-1)^{j+m} + 1 \right] \quad (16)$$

are clearly zero when $j + m$ is odd, corresponding to a consecutive sequence of odd- and even-numbered beam modes. When $j + m$ is even, corresponding to all odd- or all even-numbered modes, the right-hand side of equation (16) reduces to

$$\frac{8N_j^2 N_m^2 (\gamma_j N_j - \gamma_m N_m)}{N_m^4 - N_j^4}$$

A similar relation, of course, holds for the circumferential integrals $\int_0^{\alpha a} Y'_k Y'_n ds$ and $\int_0^{\alpha a} Y_k Y''_n ds$. The matrix elements in equations (14) with $j + m$ and $k + n$ even are given in the appendix (eqs. (A1)) for the panel with all edges clamped.

Thus, for a curved panel with opposite edges simply supported, no modal coupling occurs, and only the elements with subscripts mn are retained in equations (14). For opposite edges fully clamped or free, modal coupling occurs for a sequence of either odd- or even-numbered modes. In these latter cases, it is reasonable to expect the spread between successive odd or even eigenvalues and the differences between corresponding beam mode shapes (for example, between N_j and N_{j+2} and between X_j and X_{j+2}) to be large enough for the coupling effect of several of these modes on the

lowest panel modes to be small. The work of Young and Warburton on flat-panel vibrations (refs. 9 and 10) indicates a negligible effect on frequency due to increasing the number of mode-shape products for plates with not only clamped edges but with other edge conditions as well. A negligible effect was also found in the present study for the curved panels of references 7 and 8 (the panels being assumed to be fully clamped at all edges) due to the coupling of beam modes, j and m being 1, 3, or 5. (The comparison is made in table I between the frequencies calculated by equations (A2) and those calculated by the uncoupled frequency equations (eqs. (17) and (20)) given in the following sections and based on single-term beam-mode approximations to each displacement series. Equations (A2) are based on equation (9), and the calculations with j and m being 1, 3, or 5 were actually made with minor modifications in the torsional stiffness terms. It is assumed that a similar comparison based on equations (A1) would show the same effect.)

General uncoupled shallow-shell frequency equation. - When the off-diagonal matrix elements vanish because of the particular edge conditions and modal combinations just specified and when only one beam-mode function is used to approximate the longitudinal component of each displacement series, equations (14) may, by successive interchanges of matrix rows and columns in equation (11), be shown to reduce to the following simple equation:

$$\Delta = \Delta_I + \Delta_E \quad (17)$$

where

$$\Delta_I = \frac{D}{CM_{mn}} \left[I_2 + I_3 + 2\mu I_6 + 2(1 - \mu)I_1 \right] \quad (17a)$$

and

$$\Delta_E = \frac{1}{a^2} \left\{ 1 - \frac{I_5^2 \left(I_2 + \frac{1-\mu}{2} I_1 \right) - 2\mu I_4 I_5 \left(\mu I_6 + \frac{1-\mu}{2} I_1 \right) + (\mu I_4)^2 \left(I_3 + \frac{1-\mu}{2} I_1 \right)}{M_{mn} \left[\left(I_2 + \frac{1-\mu}{2} I_1 \right) \left(I_3 + \frac{1-\mu}{2} I_1 \right) - \left(\mu I_6 + \frac{1-\mu}{2} I_1 \right)^2 \right]} \right\} \quad (17b)$$

The subscripts I and E denote inextensional and extensional, respectively, and equation (17a) is a general form of the equation for flat-panel vibrations. The quantities I_1, \dots, I_6 represent the double integrals in the matrix elements $A_{mn}, E_{mn}, \dots, K_{mn}$ and are listed in table II.

Curved panel clamped at all edges.— The beam vibration functions approximating the X- and Y-components of a curved panel clamped at all edges are given by

$$\left. \begin{aligned} X_{j,m} &= \cosh N_{j,m}x - \cos N_{j,m}x - \gamma_{j,m}(\sinh N_{j,m}x - \sin N_{j,m}x) \\ Y_{k,n} &= \cosh N_{k,n}s - \cos N_{k,n}s - \gamma_{k,n}(\sinh N_{k,n}s - \sin N_{k,n}s) \end{aligned} \right\} \quad (18)$$

which satisfy the conditions of zero displacements and zero slopes (that is, $w_x = w_s = 0$) at all edges. (It is noted that eqs. (18) also give $v_x = u_y = 0$ at the edges and thereby imply that the in-plane stress resultant N_{xy} is 0 at the edges in contradiction with the other clamped-edge conditions. This inconsistency is believed to have a small effect on the w-mode frequencies and can be removed by other choices of modal functions.) Values of $N_{j,m}$ and $N_{k,n}$ are obtained from the equations

$$\left. \begin{aligned} \cosh \beta \cos \beta &= 1 & (\beta = N_{j,m}l \text{ or } N_{k,n}\alpha a) \\ \gamma &= \frac{\cosh \beta - \cos \beta}{\sinh \beta - \sin \beta} \end{aligned} \right\} \quad (19)$$

and are tabulated in various places in the literature. In the present study, they were taken from reference 15.

With the X- and Y-components given by equations (18) and (19), the integrals in equations (14) and (17) may be evaluated by use of reference 14, and the frequencies of a curved panel clamped at all edges may be obtained. When $j + m$ and $k + n$ are odd and only one term is retained in each series, equations (17a) and (17b) become

$$\Delta_I = \frac{D}{C} \left(N_m^4 + 2 \frac{\bar{N}_m \bar{N}_n}{\alpha a l} + N_n^4 \right) \quad (20a)$$

and

$$\begin{aligned} \Delta_E &= \frac{1/a^2}{(N_m N_n)^4 + \frac{1-\mu}{2} \frac{\bar{N}_m \bar{N}_n}{\alpha a l} (N_m^4 + N_n^4) - \mu \left(\frac{\bar{N}_m \bar{N}_n}{\alpha a l} \right)^2} \left\{ (N_m N_n)^4 \left[1 - \left(\frac{\bar{N}_n}{N_n} \right)^2 \left(\frac{1}{N_n \alpha a} \right)^2 - \left(\frac{\bar{N}_m}{N_m} \right)^2 \left(\frac{\mu}{N_m l} \right)^2 \right] \right. \\ &\quad \left. + \frac{1-\mu}{2} \frac{\bar{N}_m \bar{N}_n}{\alpha a l} \left[N_m^2 \left(N_m^2 - \left(\frac{\mu \bar{N}_m}{N_m l} \right)^2 \right) + N_n^2 \left(N_n^2 - \left(\frac{\bar{N}_n}{N_n \alpha a} \right)^2 \right) \right] + \mu^2 \left(\frac{\bar{N}_m \bar{N}_n}{\alpha a l} \right)^2 \right\} \quad (20b) \end{aligned}$$

where $\bar{N}_m = \gamma_m N_m (\gamma_m N_m l - 2)$ and $\bar{N}_n = \gamma_n N_n (\gamma_n \alpha a - 2)$. Values for the double integrals I_1, \dots, I_6 are listed in table II for the all-clamped edge condition.

Curved panel with all edges simply supported.- The X- and Y-components of a curved panel simply supported at all edges are given by equations (15) which satisfy the following edge conditions:

$$\begin{aligned}
 u &= 0 & (s = 0; \quad s = \alpha a) \\
 N_y &= 0 & (s = 0; \quad s = \alpha a) \\
 v &= 0 & (x = 0; \quad x = l) \\
 N_x &= 0 & (x = 0; \quad x = l) \\
 w &= 0 & (\text{All edges}) \\
 w_{xx} &= 0 & (x = 0; \quad x = l) \\
 w_{ss} &= 0 & (s = 0; \quad s = \alpha a)
 \end{aligned}$$

where N_x is the longitudinal membrane stress resultant and N_y the circumferential membrane stress resultant. Between the straight edges ($s = 0, \quad s = \alpha a$) the panel is free to move longitudinally (u-direction), and between the curved edges ($x = 0, \quad x = l$) the panel is free to move circumferentially (v-direction).

With the X- and Y-components given by equations (15), the integrals in equations (17) are evaluated (see table II), and the frequency equation reduces to

$$\Delta = \frac{D\pi^4}{C} \left[\left(\frac{m}{l} \right)^2 + \left(\frac{n}{\alpha a} \right)^2 \right]^2 + \frac{\frac{1}{a^2} \left(\frac{m}{l} \right)^4 (1 - \mu^2)}{\left[\left(\frac{m}{l} \right)^2 + \left(\frac{n}{\alpha a} \right)^2 \right]^2} \quad (21)$$

which is essentially of the same form as that given by Oniashvili in reference 4 (p. 22) and also by Berry and Reissner in reference 13 for elements of thin shallow shells.

An evaluation of shallow-shell assumptions.- As noted earlier, beam vibration functions could also be used in the complete frequency equation (eq. (9)), although it is more consistent, for panels of small curvature, to confine their use to equation (11). The use of beam functions in equation (9) amounts to an evaluation of the basic shallow-shell assumptions in equation (11), namely, the neglect of in-plane inertias and the

neglect of circumferential and longitudinal contributions to the changes of curvature κ_2 and κ_{12} (as indicated in eqs. (3)). Retention of in-plane inertias leads to two more sets of frequencies for each modal combination than are obtained from equation (11). These additional frequencies are associated with in-plane shell vibrations and are very much higher than the remaining set of frequencies which are associated with normal or radial vibrations. Moreover, the effect of these in-plane modes on the radial modes is negligible, as may be shown by the fact that frequencies calculated by equations (17), (20), and (21) are essentially the same as those calculated by equation (A3). Equation (A3) is a general uncoupled frequency equation that can be reduced from equation (9) in the same way that equation (17) was obtained from equation (11).

COMPARISON BETWEEN THEORY AND EXPERIMENT

The experimental frequencies given in references 6 to 8 are compared in tables III and IV and in figures 2 to 5 with those calculated by equations (17), (20), and (21). (The data actually presented in ref. 6 are supplemented by unpublished data from Flight Dynamic Laboratory, U.S. Air Force, that were obtained as part of the same investigation.) Pertinent features of the experiments are described first, and are followed by comparisons between theoretical and experimental frequencies, both for the limiting case of flat panels and for curved panels, the effects of nonzero curvature and edge support conditions being considered together. Consideration is next given to the effects of panel thickness.

Vibration Experiments of Curved Panels

The panels of references 6 to 8 were made of aluminum alloy and, in most of the tests, were secured to support frames, as indicated in figure 1, by simple lap attachments with closely spaced bolts (for example, $\frac{1}{8}$ inch in diameter and spaced $1\frac{1}{16}$ inches on centers in ref. 7; $\frac{3}{16}$ inch in diameter and spaced $1\frac{1}{2}$ inches on centers in ref. 8). In some of the tests in reference 6, the edge supports were reinforced by use of an additional attachment frame fastened, as shown schematically in figure 1, to achieve greater clamping action symmetrically applied with respect to the middle surface of the panel, in contrast to the unsymmetrical clamping action of the lap attachment. All the curved panels in references 6 to 8 were formed to their supports and were not rolled. The panels of reference 6 were 0.028 inch (0.071 cm) and 0.048 inch (0.12 cm) thick and had unsupported dimensions of 11 inches (27.94 cm) by 9 inches (22.86 cm). These panels were very nearly the same size as those of reference 7, which were $\frac{5}{8}$ inch (1.59 cm) longer on each edge and had a thickness of 0.032 inch (0.081 cm). The panels of

reference 8 were 0.020 inch (0.051 cm), 0.032 inch (0.081 cm), and 0.040 inch (0.10 cm) thick and were square with an unsupported dimension of about 17.5 inches* (44.45 cm) on a side.

Flat Panels

Experimental and theoretical frequencies, calculated by means of equation (20a), are shown in the left-hand plots of figures 2 and 4 to be in very good agreement for the flat rectangular panels of references 6 and 7, on the basis of fully clamped edges. This good agreement (which is also shown in ref. 7 on the basis of Warburton's equations of ref. 10) suggests that the closely spaced bolts securing this panel to its support frame provided sufficient edge fixity for adequate representation of fully clamped edges. Good agreement is also shown in figure 5 for the flat square panels of reference 8, also under conditions of ideally clamped edges approximated by means of closely spaced bolts.

Curved Panels

The effects of curvature on panel frequencies are shown in the middle and right-hand plots of figures 2, 4, and 5 for both clamped and simply supported edges. As curvature increased (or radius decreased), both calculated and measured frequencies of the lower modes experienced greater increases than did the higher mode frequencies, and, as may be seen in figure 2(a), minimum frequencies tended to occur at circumferential mode numbers greater than $n = 1$. This behavior is attributed to the influence of the membrane contribution to the frequency (that is, the Δ_E component in eqs. (17b) and (20b) and the second term in eq. (21)). For example, in equation (21) for the simply supported curved panel, the second term predominates at low values of n but clearly diminishes as n increases. The first term, which is the bending frequency contribution, predominates as n increases. These trends are essentially the same as the well-known ones for the complete cylindrical shell as discussed by Arnold and Warburton in reference 16.

Another somewhat broader view of the effects of curvature and edge fixity is afforded by figure 3 for all combinations of mode numbers up to and including m and n

*The length actually used in the present frequency calculation was 17.0 inches (43.18 cm) which is the free length between the edges of the support frame, whereas 17.5 inches (44.45 cm) is a so-called "effective" length (ref. 7) that includes a little less than half the distance between the inside free edge of the support frame and the center-line of the row of mounting bolts. Calculated frequencies based on 17.5 inches (44.45 cm) were no more than 6 percent lower than those based on 17.0 inches (43.18 cm) for the larger values of n ($n = 7$) for either simply supported or clamped-edge panels.

of 5 for the rectangular panels of reference 6. Here, in terms of a dimensionless frequency parameter shown as a function of the ratio of axial to circumferential wave lengths, the gridwork pattern of figure 3(a) becomes more distorted with increasing curvature. Also, the diminishing effects of edge fixity are evident in the progressively steeper trends in both solid and dashed gridworks in the left-hand portions of the plots as m increases.

Effects of edge fixity.- Most of the experimental frequencies of the curved panels of references 6 to 8 fell somewhere between the calculated frequencies based on all edges fully clamped and all edges simply supported. The extent of the actual edge clamping action, of course, determines how close the experimental frequency trends were to either upper or lower calculated frequency bounds. At low values of n , as the panel curvature increased, the experimental frequencies were generally closer to the lower bounds, for which all edges were assumed to be simply supported. (See figs. 4(a) and 5.) As n , and also m , increased, the experimental frequencies showed some tendency to move closer to the upper bounds (all edges assumed clamped). This tendency was more evident for the rectangular panels of reference 7 and the square panels of reference 8 than it was for the rectangular panels of reference 6. These experimental and calculated trends suggest that the lap attachments and closely spaced mounting bolts may not have been sufficient to restrain fully the in-plane displacements of the panel at its edges for low n , but evidently became more satisfactory in this respect as n increased and the predominant bending energy required less clamping action.

Reinforcement of the panel edges by means of the additional clamping frame in reference 6 resulted in increases in the experimental frequencies by as much as 12 percent (for $m, n = 1, 5$ with $a = 96$ inches (243.84 cm) and $h = 0.048$ inch (0.12 cm) in figs. 2 and 3 and table III(b)). The agreement between these frequencies and those of the upper calculated frequency bounds is seen to be greatly improved for all modes except $m, n = 1, 1$ and $1, 2$, for which even this additional clamping action may not have been sufficient to restrain the in-plane edge displacements in these low modes.

In view of the dominant effect of the circumferential strain ϵ_2 noted earlier in the general derivation of the equations, it is reasonable to expect a greater increase in experimental frequencies with heavier reinforcement along the straight edges than along the curved edges. A possible indication of such a result may be seen in the relatively small reduction in upper clamped-edge frequencies due to setting the longitudinal strain $\epsilon_1 = 0$, in contrast to the complete elimination of the membrane frequency contribution when $\epsilon_2 = 0$, as shown in figures 4(a) and 4(b). For the lower frequency boundary, with all edges assumed simply supported (which involves unrestrained circumferential edge displacements as previously noted), membrane effects were eliminated by putting

either ϵ_1 or ϵ_2 equal to zero. As shown in figure 4, all other frequencies fell above this lower boundary.

Remarks on unbounded experimental frequencies.- Although most of the experimental frequencies fell within upper and lower calculated frequency boundaries, enough values lay outside this range to merit some discussion. Although no fully satisfactory explanation of these modes appears to be possible, some observations are offered here, based, in part, on examination of the experimental nodal patterns presented in reference 6.

As many as 10 of the experimental frequencies of the 0.028-inch (0.071 cm) panels of reference 6 are seen in figure 2 and table III to be higher than the corresponding calculated frequencies with all edges assumed fully clamped. Comparison of the nodal patterns of these modes with those for the 0.048-inch (0.12 cm) panels reveals significant enough differences in mode shape to indicate the possible presence or influence of other modes, particularly for those modes with experimental frequencies about 11 percent and 20 percent higher than calculated upper bound frequencies (that is, $m, n = 3, 1$ for $a = 72$ inches (182.9 cm) and 96 inches (243.84 cm), respectively). (The data in ref. 6 are given for nominal values of 0.051 inch and 0.032 inch. The actual measured thicknesses in the supplementary unpublished data included in the present paper are 0.048 inch and 0.028 inch.)

On the lower side of the calculated frequency range, five of the experimental frequencies of references 7 and 8 were lower than the calculated lower bound frequencies with all edges assumed simply supported. The largest discrepancies may be seen in figure 4(b) for $m, n = 3, 1$ and $a = 96$ inches (243.84 cm) and in figure 5 for $m, n = 1, 2$ and $a = 48$ inches (121.92 cm), in which experimental frequencies were anywhere from 8 percent (fig. 4(b)) to about 40 percent (fig. 5) lower than the corresponding calculated lower bound frequencies. In these cases, the actual edge conditions evidently did not satisfy fully the requirements of simply supported edges with membrane effects included, and the lower bounds became the calculated trends in inextensional frequencies.

Effects of panel thickness.- The effects of panel thickness are shown in figures 2 and 3 for the rectangular panels of reference 6 and in figure 5 for the square panels of reference 8. Increasing thickness clearly resulted in greater increases in the frequencies of modes for higher values of n than for lower values of n as shown in figures 2 and 5. As both m and n increased and inextensional effects became predominant, the calculated frequencies became more nearly proportional to thickness, as is indicated by the nearly equal values of dimensionless frequencies in the upper parts of figure 3 for both thicknesses. This relation holds over a somewhat larger range of m and n for calculated frequencies with simply supported edges than for those with clamped edges.

CONCLUDING REMARKS

The energy method employing the Rayleigh-Ritz procedure is applied to the vibration of cylindrically curved rectangular and square panels for which experimental vibration data are known. General frequency equations are derived and applied to panels of small curvature with the mode shapes approximated by products of beam vibration functions satisfying certain geometrical edge conditions in both longitudinal and circumferential directions. This application leads to simplified Rayleigh-type frequency equations that reduce to those obtained previously by other investigators for flat panels and for curved panels with all edges simply supported. In the present study, these equations proved to be more satisfactory for certain modal combinations and edge conditions than for others.

Most of the measured frequencies were bracketed by calculated frequencies with all edges assumed clamped for the upper bound and all edges assumed simply supported for the lower bound. Comparable frequencies were measured on panels of the same material and essentially the same size in two investigations conducted independently. At low-order circumferential modes, the measured frequencies were generally closer to the lower calculated frequency bound, and as the order of the circumferential mode increased, measured frequencies showed some tendency to move closer to the upper calculated frequency bound. This behavior is attributed partly to membrane effects (due to panel curvature) and partly to complicated edge conditions (due to the use of bolted simple lap attachments) that could not be adequately represented by theory. Comparison of experimental frequencies with inextensional frequencies, calculated with longitudinal and/or circumferential membrane strains omitted, indicated that the actual panel mountings may have provided greater edge fixity along curved rather than along straight edges.

Increasing panel thickness resulted in greater increases in the frequencies of modes for higher circumferential mode numbers than for lower mode numbers.

Further efforts to bring theoretical and experimental frequencies into closer agreement should include an examination of the effects of modal functions other than beam functions, calculations by other methods of analysis (such as methods of finite differences and/or finite elements), and vibration tests of curved panels with edges designed to satisfy ideal simply supported or clamped conditions as closely as possible.

Langley Research Center,
National Aeronautics and Space Administration,
Langley Station, Hampton, Va., July 22, 1966,
124-08-05-02-23.

APPENDIX

SUPPLEMENTARY FREQUENCY EQUATIONS BASED ON THE RAYLEIGH-RITZ VIBRATION ANALYSIS FOR CURVED PANELS

This appendix contains the matrix elements of additional frequency equations evolving from the general vibration analysis presented in the main text and with elementary beam vibration functions approximating longitudinal and circumferential components of the panel mode shapes. The first two of these equations apply to the vibration of curved panels with all edges fully clamped for a sequence of either odd- or even-numbered modes. Another frequency equation included is a general uncoupled equation based on the complete Rayleigh-Ritz vibration analysis represented by equation (9) and obtained under the same conditions specified in reducing equations (14) to equation (17).

Rayleigh-Ritz Frequency Equations for the Vibration of Curved Panels With All Edges Fully Clamped

On the basis of forms 16 and 20 of reference 14, as illustrated by equation (16), the shallow-shell matrix elements in equations (14) may be written as follows for a curved panel clamped at all edges, with $j + m$ and $k + n$ even:

$$\left. \begin{aligned}
 A_{pq} = A_{mn} &= \frac{1}{l\alpha a} \left[\left(\frac{\alpha a}{l} \right)^2 (N_m l)^4 + \frac{1-\mu}{2} \bar{N}_m \bar{N}_n l \alpha a \right] & (j = m; \quad k = n) \\
 A_{pq} = F_{pq} &= \frac{1-\mu}{2} \left[\frac{64 (N_j N_m N_k N_n)^2 (\gamma_j N_j - \gamma_m N_m) (\gamma_k N_k - \gamma_n N_n)}{(N_m^4 - N_j^4) (N_n^4 - N_k^4)} \right] & (j \neq m; \quad k \neq n) \\
 E_{pq} = E_{mn} &= \bar{N}_m \bar{N}_n \left(\frac{1+\mu}{2} \right) & (j = m; \quad k = n) \\
 E_{pq} &= \frac{1+\mu}{1-\mu} A_{pq} & (j \neq m; \quad k \neq n) \\
 G_{pq} = G_{mn} &= -\frac{\mu}{a} \bar{N}_m \alpha a & (j = m; \quad k = n)
 \end{aligned} \right\} \quad (A1)$$

(Equation continued on next page)

APPENDIX

$$\begin{aligned}
 G_{pq} = G_{jm} &= -\frac{\mu}{a} \frac{8N_j^2 N_m^2 (\gamma_j N_j - \gamma_m N_m)}{N_m^4 - N_j^4} \alpha a & (j \neq m; \quad k = n) \\
 G_{pq} &= 0 & (k \neq n) \\
 F_{pq} = F_{mn} &= \frac{1}{l \alpha a} \left[\left(\frac{l}{\alpha a} \right)^2 (N_n \alpha a)^4 + \frac{1 - \mu}{2} \bar{N}_m \bar{N}_n l \alpha a \right] & (j = m; \quad k = n) \\
 J_{pq} = J_{mn} &= -\frac{\bar{N}_n l}{a} & (j = m; \quad k = n) \\
 J_{pq} = J_{kn} &= -\frac{l}{a} \frac{8N_k^2 N_n^2 (\gamma_k N_k - \gamma_n N_n)}{N_n^4 - N_k^4} & (j = m; \quad k \neq n) \\
 J_{pq} &= 0 & (j \neq m) \\
 K_{pq} = K_{mn} &= l \alpha a \left[\frac{1}{a^2} + \frac{D}{C} \left(N_m^4 + 2 \frac{\bar{N}_m \bar{N}_n}{l \alpha a} + N_n^4 \right) \right] & (j = m; \quad k = n) \\
 K_{pq} &= \frac{4}{1 - \mu} \frac{D}{C} A_{pq} & (j \neq m; \quad k \neq n) \\
 M_{pq} = M_{mn} &= l \alpha a & (j = m; \quad k = n) \\
 M_{pq} &= 0 & (j \neq m \quad \text{and/or} \quad k \neq n)
 \end{aligned} \tag{A1}$$

If elementary beam vibration functions are used in equation (9), a set of matrix elements similar to, and more complete than, those of equations (14) is obtained. These elements are given in the following equation, first in general form and then for a curved panel clamped at all edges with $j + m$ and $k + n$ even:

APPENDIX

$$\begin{aligned}
 A_{pq} &= A_{mn} = \int_0^{\alpha a} \int_0^l (x_m'' y_n'')^2 dx ds + \frac{1-\mu}{2} \left(1 + \frac{D}{4a^2 C}\right) \int_0^{\alpha a} \int_0^l (x_m' y_n')^2 dx ds & (j = m; \quad k = n) \\
 A_{pq} &= \frac{1-\mu}{2} \left(1 + \frac{D}{4a^2 C}\right) \int_0^{\alpha a} \int_0^l x_j' x_m' y_k' y_n' dx ds & (j \neq m \quad \text{and/or} \quad k \neq n) \\
 B_{pq} &= B_{mn} = \int_0^{\alpha a} \int_0^l (x_m' y_n')^2 dx ds & (j = m; \quad k = n) \\
 B_{pq} &= B_{jm} = \int_0^{\alpha a} \int_0^l x_j' x_m' y_n'^2 dx ds & (j \neq m; \quad k = n) \\
 B_{pq} &= 0 & (k \neq n) \\
 E_{pq} &= E_{mn} = \mu \int_0^{\alpha a} \int_0^l x_m'' x_m' y_n' y_n'' dx ds + \frac{1-\mu}{2} \left(1 - \frac{3D}{4a^2 C}\right) \int_0^{\alpha a} \int_0^l (x_m' y_n')^2 dx ds & (j = m; \quad k = n) \\
 E_{pq} &= \mu \int_0^{\alpha a} \int_0^l x_j' x_m' y_k' y_n'' dx ds + \frac{1-\mu}{2} \left(1 - \frac{3D}{4a^2 C}\right) \int_0^{\alpha a} \int_0^l x_j' x_m' y_k' y_n' dx ds & (j \neq m; \quad k \neq n) \\
 G_{pq} &= G_{mn} = \frac{1}{a} \left[\mu \int_0^{\alpha a} \int_0^l x_m'' x_m' y_n'^2 dx ds + \frac{1-\mu}{2} \frac{D}{C} \int_0^{\alpha a} \int_0^l (x_m' y_n')^2 dx ds \right] & (j = m; \quad k = n) \\
 G_{pq} &= G_{jm} = \frac{1}{a} \left[\mu \int_0^{\alpha a} \int_0^l x_j' x_m' y_n'^2 dx ds + \frac{1-\mu}{2} \frac{D}{C} \int_0^{\alpha a} \int_0^l x_j' x_m' (y_n')^2 dx ds \right] & (j \neq m; \quad k = n) \\
 G_{pq} &= \frac{1-\mu}{2a} \frac{D}{C} \int_0^{\alpha a} \int_0^l x_j' x_m' y_k' y_n' dx ds & (k \neq n) \\
 F_{pq} &= F_{mn} = \left(1 + \frac{D}{a^2 C}\right) \int_0^{\alpha a} \int_0^l (x_m' y_n')^2 dx ds + \frac{1-\mu}{2} \left(1 + \frac{9D}{4a^2 C}\right) \int_0^{\alpha a} \int_0^l (x_m' y_n')^2 dx ds & (j = m; \quad k = n) \\
 F_{pq} &= \frac{1-\mu}{2} \left(1 + \frac{9D}{4a^2 C}\right) \int_0^{\alpha a} \int_0^l x_j' x_m' y_k' y_n' dx ds & (j \neq m \quad \text{and/or} \quad k \neq n) \\
 H_{pq} &= H_{mn} = \int_0^{\alpha a} \int_0^l (x_m' y_n')^2 dx ds & (j = m; \quad k = n) \\
 H_{pq} &= H_{mn} = \int_0^{\alpha a} \int_0^l x_m'^2 y_k' y_n' dx ds & (j = m; \quad k \neq n) \\
 H_{pq} &= 0 & (j \neq m) \\
 J_{pq} &= J_{mn} = \frac{1}{a} \left\{ \int_0^{\alpha a} \int_0^l x_m'^2 y_n'' y_n' dx ds - \frac{D}{C} \left[\mu \int_0^{\alpha a} \int_0^l x_m x_m'' y_n' y_n' dx ds + \int_0^{\alpha a} \int_0^l (x_m' y_n'')^2 dx ds + \frac{3(1-\mu)}{2} \int_0^{\alpha a} \int_0^l (x_m' y_n')^2 dx ds \right] \right\} & (j = m; \quad k = n) \\
 J_{pq} &= J_{kn} = \frac{1}{a} \left\{ \int_0^{\alpha a} \int_0^l x_m'^2 y_k'' y_n' dx ds - \frac{D}{C} \left[\mu \int_0^{\alpha a} \int_0^l x_m x_m'' y_k' y_n' dx ds + \frac{3(1-\mu)}{2} \int_0^{\alpha a} \int_0^l (x_m')^2 y_k' y_n' dx ds \right] \right\} & (j = m; \quad k \neq n) \\
 J_{pq} &= J_{jm} = -\frac{D}{aC} \left[\mu \int_0^{\alpha a} \int_0^l x_j x_m'' y_n' y_n' dx ds + \frac{3(1-\mu)}{2} \int_0^{\alpha a} \int_0^l x_j' x_m' (y_n')^2 dx ds \right] & (j \neq m; \quad k = n) \\
 K_{pq} &= K_{mn} = \frac{1}{a^2} \int_0^{\alpha a} \int_0^l (x_m' y_n'')^2 dx ds + \frac{D}{C} \left[\int_0^{\alpha a} \int_0^l (x_m'' y_n'')^2 dx ds + 2\mu \int_0^{\alpha a} \int_0^l x_m x_m'' y_n' y_n' dx ds \right. \\
 &\quad \left. + \int_0^{\alpha a} \int_0^l (x_m' y_n'')^2 dx ds + 2(1-\mu) \int_0^{\alpha a} \int_0^l (x_m' y_n')^2 dx ds \right] & (j = m; \quad k = n) \\
 K_{pq} &= \frac{D}{C} \left[\mu \int_0^{\alpha a} \int_0^l (x_j x_m'' y_k' y_n' + x_j' x_m' y_k' y_n'') dx ds + 2(1-\mu) \int_0^{\alpha a} \int_0^l x_j' x_m' y_k' y_n' dx ds \right] & (j \neq m; \quad k \neq n) \\
 M_{pq} &= M_{mn} = \int_0^{\alpha a} \int_0^l (x_m' y_n')^2 dx ds & (j = m; \quad k = n) \\
 M_{pq} &= 0 & (j \neq m \quad \text{and/or} \quad k \neq n)
 \end{aligned}
 \tag{A2a}$$

APPENDIX

For a curved edge with all edges clamped and $j + m$ and $k + n$ even, these elements become

$$\begin{aligned}
 A_{mn} &= \frac{1}{l\alpha a} \left[\left(\frac{\alpha a}{l} \right)^2 (N_m l)^4 + \frac{1-\mu}{2} \left(1 + \frac{D}{4a^2 C} \right) \bar{N}_m \bar{N}_n l \alpha a \right] & (j = m; k = n) \\
 A_{pq} &= \frac{1-\mu}{2} \left(1 + \frac{D}{4a^2 C} \right) \frac{64(N_j N_m N_k N_n)^2 (\gamma_j N_j - \gamma_m N_m)(\gamma_k N_k - \gamma_n N_n)}{(N_m^4 - N_j^4)(N_n^4 - N_k^4)} & (j \neq m; k \neq n) \\
 B_{mn} &= \bar{N}_m \alpha a & (j = m; k = n) \\
 B_{jm} &= \frac{8(N_j N_m)^2 (\gamma_j N_j - \gamma_m N_m)}{N_m^4 - N_j^4} \alpha a & (j \neq m; k = n) \\
 E_{mn} &= \bar{N}_m \bar{N}_n \left[\mu + \frac{1-\mu}{2} \left(1 - \frac{3D}{4a^2 C} \right) \right] & (j = m; k = n) \\
 E_{pq} &= \left[\mu + \frac{1-\mu}{2} \left(1 - \frac{3D}{4a^2 C} \right) \right] \frac{64(N_j N_m N_k N_n)^2 (\gamma_j N_j - \gamma_m N_m)(\gamma_k N_k - \gamma_n N_n)}{(N_m^4 - N_j^4)(N_n^4 - N_k^4)} & (j \neq m; k \neq n) \\
 G_{mn} &= \frac{\bar{N}_m}{a} \left[-\mu \alpha a + \bar{N}_n \frac{D}{2C} (1 - \mu) \right] & (j = m; k = n) \\
 G_{jm} &= \frac{8N_j^2 N_m^2 (\gamma_j N_j - \gamma_m N_m)}{a(N_m^4 - N_j^4)} \left(-\mu \alpha a + \frac{1-\mu}{2} \frac{D}{C} \bar{N}_n \right) & (j \neq m; k = n) \\
 G_{kn} &= \frac{1-\mu}{2a} \frac{D}{C} \left[\frac{64(N_j N_m N_k N_n)^2 (\gamma_j N_j - \gamma_m N_m)(\gamma_k N_k - \gamma_n N_n)}{(N_m^4 - N_j^4)(N_n^4 - N_k^4)} \right] & (j \neq m; k \neq n) \\
 F_{mn} &= \frac{1}{l\alpha a} \left[\left(1 + \frac{D}{4a^2 C} \right) \left(\frac{l}{\alpha a} \right)^2 (N_n \alpha a)^4 + \frac{1-\mu}{2} \left(1 + \frac{9D}{4a^2 C} \right) \bar{N}_m \bar{N}_n l \alpha a \right] & (j = m; k = n) \\
 F_{pq} &= \frac{1 + \frac{9D}{4a^2 C}}{1 + \frac{D}{4a^2 C}} A_{pq} & (j \neq m; k \neq n) \\
 H_{mn} &= \bar{N}_n l & (j = m; k = n) \\
 H_{kn} &= \frac{8(N_k N_n)^2 (\gamma_k N_k - \gamma_n N_n)}{N_n^4 - N_k^4} l & (j = m; k \neq n) \\
 J_{mn} &= -\frac{1}{a} \left\{ \bar{N}_n l + \frac{D}{Cl\alpha a} \left[\left(\frac{l}{\alpha a} \right)^2 (N_n \alpha a)^4 + \frac{3-\mu}{2} \bar{N}_m \bar{N}_n l \alpha a \right] \right\} & (j = m; k = n) \\
 J_{kn} &= \frac{-8(N_k N_n)^2 (\gamma_k N_k - \gamma_n N_n)}{a(N_n^4 - N_k^4)} \left[l + \frac{D}{C} \bar{N}_m \left(\frac{3-\mu}{2} \right) \right] & (j = m; k \neq n) \\
 J_{jm} &= -\frac{D\bar{N}_n}{aC} \frac{8N_j^2 N_m^2 (\gamma_j N_j - \gamma_m N_m)}{N_m^4 - N_j^4} \left(\frac{3-\mu}{2} \right) & (j \neq m; k = n) \\
 K_{mn} &= l\alpha a \left[\frac{1}{a^2} + \frac{D}{C} \left(N_m^4 + 2 \frac{\bar{N}_m \bar{N}_n}{l\alpha a} + N_n^4 \right) \right] & (j = m; k = n) \\
 K_{pq} &= \frac{4}{1-\mu} \frac{D/C}{1 + \frac{D}{4a^2 C}} A_{pq} & (j \neq m; k \neq n) \\
 M_{mn} &= l\alpha a & (j = m; k = n) \\
 M_{pq} &= 0 & (j \neq m; k \neq n)
 \end{aligned} \tag{A2b}$$

APPENDIX

As is noted in the main body of the paper, the frequencies calculated by using equations (A2) for $j, m = 1, 3, 5$ were made with minor modifications in the torsional stiffness terms. Specifically, the terms involving $\frac{D}{C}$ were omitted from the A-, E-, and G-matrices, $9/4$ was replaced by 4 in the F-matrix, $\frac{3-\mu}{2}$ by $2-\mu$ in the J-elements (eqs. (A2b)). These changes correspond to replacing κ_{12} in equations (2) by $\kappa_{12} = -w_{xs} + \frac{v_x}{a}$, which is the torsional change of curvature given by Love in reference 17 (with w oriented outward as in fig. 1 instead of inward as in ref. 17). Frequency calculations not included in this paper indicated that the effect of these minor modifications was negligible.

General Uncoupled Frequency Equation

When the off-diagonal matrix elements in equations (A2a) vanish for opposite edges fully clamped or free (for the elastic modes) and for $j + m$ or $k + n$ odd, with only one beam-mode function retained in each displacement series, an uncoupled frequency equation may be obtained, just as the uncoupled shallow-shell frequency equation (eq. (17)) was obtained from equations (14) in the main text. This simplified equation may be written in the following determinantal form

$$\begin{vmatrix} A_{mn} - \Delta B_{mn} & E_{mn} & G_{mn} \\ E_{mn} & F_{mn} - \Delta H_{mn} & J_{mn} \\ G_{mn} & J_{mn} & K_{mn} - \Delta M_{mn} \end{vmatrix} = 0 \quad (A3)$$

where each of the determinant elements is given in equations (A2a) for $j = m$ and $k = n$ and may also be expressed as

$$A_{mn} = I_2 + \frac{1-\mu}{2} \left(1 + \frac{D}{4a^2 C} \right) I_1$$

$$E_{mn} = \mu I_6 + \frac{1-\mu}{2} \left(1 - \frac{3D}{4a^2 C} \right) I_1$$

$$G_{mn} = \frac{1}{a} \left[\mu I_4 + \frac{D}{2C} (1 - \mu) I_1 \right]$$

APPENDIX

$$F_{mn} = \left(1 + \frac{D}{a^2 C}\right) I_3 + \frac{1 - \mu}{2} \left(1 + \frac{9D}{4a^2 C}\right) I_1$$

$$J_{mn} = \frac{1}{a} \left\{ I_5 - \frac{D}{C} \left[I_3 + \mu I_6 + \frac{3}{2} (1 - \mu) I_1 \right] \right\}$$

$$K_{mn} = \frac{M_{mn}}{a^2} + \frac{D}{C} \left[I_2 + I_3 + 2\mu I_6 + 2(1 - \mu) I_1 \right]$$

where B_{mn} , H_{mn} , M_{mn} , and I_1 to I_6 are listed in table II.

REFERENCES

1. Reissner, Eric: On Transverse Vibrations of Thin, Shallow Elastic Shells. *Quart. Appl. Math.*, vol. XIII, no. 2, July 1955, pp. 169-176.
2. Palmer, P. J.: The Natural Frequency of Vibration of Curved Rectangular Plates. *Aeron. Quart.*, vol. V, pt. 2, July 1954, pp. 101-110.
3. Forsberg, Kevin: Influence of Boundary Conditions on the Modal Characteristics of Thin Cylindrical Shells. *AIAA J.*, vol. 2, no. 12, Dec. 1964, pp. 2150-2157.
4. Oniashvili, O. D.: Certain Dynamic Problems of the Theory of Shells. Morris D. Friedman, Inc. (West Newton, Mass.), 1957.
5. Vlasov, V. Z.: General Theory of Shells and Its Applications in Engineering. NASA TT F-99, 1964.
6. Ballentine, John R.; Plumblee, Harry E.; and Schneider, Cecil W.: Sonic Fatigue in Combined Environment. AFFDL-TR-66-7, U.S. Air Force, May 1966.
7. Hess, Robert W.; Herr, Robert W.; and Mayes, William H.: A Study of the Acoustic Fatigue Characteristics of Some Flat and Curved Aluminum Panels Exposed to Random and Discrete Noise. NASA TN D-1, 1959.
8. Rucker, Carl E.: Some Experimental Effects of Curvature on Response of Simple Panels to Intense Noise. Paper presented at 67th Meeting of the Acoust. Soc. Am. (New York, N.Y.), May 1964.
9. Young, Dana: Vibration of Rectangular Plates by the Ritz Method. *J. Appl. Mech.*, vol. 17, no. 4, Dec. 1950, pp. 448-453.
10. Warburton, G. B.: The Vibration of Rectangular Plates. *Proc. Inst. Mech. Eng.* (London), vol. 168, no. 12, 1953, pp. 371-384.
11. Sanders, J. Lyell, Jr.: An Improved First-Approximation Theory for Thin Shells. NASA TR R-24, 1959.
12. Donnell, L. H.: A New Theory for the Buckling of Thin Cylinders Under Axial Compression and Bending. *Trans. ASME*, vol. 56, no. 11, Nov. 1934, pp. 795-806.
13. Berry, J. G.; and Reissner, E.: The Effect of an Internal Compressible Fluid Column on the Breathing Vibrations of a Thin Pressurized Shell. *J. Aeron. Sci.*, vol. 25, no. 5, May 1958, pp. 288-294.
14. Felgar, Robert P., Jr.: Formulas for Integrals Containing Characteristic Functions of a Vibrating Beam. Circ. No. 14, Bur. Eng. Res., Univ. of Texas, 1950.

15. Young, Dana; and Felgar, Robert P., Jr.: Tables of Characteristic Functions Representing Normal Modes of Vibration of a Beam. Publ. No. 4913, Eng. Res. Ser. No. 44, Bur. Eng. Res., Univ. of Texas, July 1, 1949.
16. Arnold, R. N.; and Warburton, G. B.: The Flexural Vibrations of Thin Cylinders. Proc (A) Inst. Mech. Engrs. (London), vol. 167, no. 1, 1953, pp. 62-74.
17. Love, A. E. H.: A Treatise on the Mathematical Theory of Elasticity. Fourth ed. (First Am. Printing), Dover Publ., 1944.

TABLE I.- EFFECT OF HIGHER ORDER LONGITUDINAL MODES ON CALCULATED
FREQUENCIES OF CURVED PANELS CLAMPED AT ALL EDGES

$$[m = 1]$$

(a) Rectangular panel, $11\frac{5}{8}$ inches \times $9\frac{5}{8}$ inches \times 0.032 inch
(29.53 cm \times 24.45 cm \times 0.081 cm) (ref. 7)

n	Frequencies, cps, for -			
	a = 96 inches (243.84 cm)		a = 48 inches (121.92 cm)	
	j = m = 1 (*)	j, m = 1, 3, 5 (**)	j = m = 1 (*)	j, m = 1, 3, 5 (**)
1	314.4	314.0	602.7	601.9
2	334.1	333.15	531.0	529.8
3	479.2	477.7	595.05	593.5
4	722.5	720.5	784.7	782.8
5	1045		1078	

(b) Square panels, 17.0 inches \times 17.0 inches (43.18 cm \times 43.18 cm)*** (ref. 8)

n	Frequencies, cps, for -			
	a = 96 inches (243.84 cm)		a = 48 inches (121.92 cm)	
	j = m = 1 (*)	j, m = 1, 3, 5 (**)	j = m = 1 (*)	j, m = 1, 3, 5 (**)
h = 0.020 inch (0.051 cm)				
1	299.5	299.0	597.3	596.3
2	245.9	245.2	484.1	482.55
3	225.55	225.0	423.7	422.6
4	232.3	231.8	393.7	393.0
5	267.1	266.5	392.9	393.0
6	326.9	326.2	421.1	420.45
7	407.7	407.0	476.9	476.2
h = 0.032 inch (0.081 cm)				
1	301.0	300.5	598.1	597.0
2	253.6	252.9	488.0	486.6
3	251.6	250.9	438.1	437.0
4	292.6	291.8	432.0	431.05
5	373.4	372.4	471.6	470.6
6	486.7	485.6	554.3	553.3
7	627.4	626.3	674.4	673.2
h = 0.040 inch (0.10 cm)				
1	302.4	301.9	598.8	597.75
2	260.5	259.8	491.65	490.25
3	273.4	272.6	451.0	449.8
4	338.8	337.8	464.5	463.4
5	449.7	448.5	534.0	532.85
6	597.4	596.1	653.6	652.3
7	776.9	775.5	815.2	813.8

*Calculated by equations (17) and (20).

**Calculated by equations (A2b) modified as noted in the appendix.

***Actual unsupported length between opposite edges of support frame.

**TABLE II. - INTEGRALS FOR MODAL FUNCTIONS IN THE FREQUENCY EQUATION
OF A CYLINDRICALLY CURVED PANEL WITH SIMPLY SUPPORTED
AND CLAMPED EDGES (BASED ON REF. 14)**

Integrals	All edges simply supported	All edges clamped
$M_{mn} = \int_0^{\alpha a} \int_0^l (X_m Y_n)^2 dx ds$	$\frac{l \alpha a}{4}$	$l \alpha a$
$B_{mn} = \int_0^{\alpha a} \int_0^l (X'_m Y_n)^2 dx ds$	$\frac{\alpha a}{4l} (m\pi)^2$	$\frac{\alpha a}{l} \gamma_m N_m l (\gamma_m N_m l - 2)$
$H_{mn} = \int_0^{\alpha a} \int_0^l (X_m Y'_n)^2 dx ds$	$\frac{l}{4\alpha a} (n\pi)^2$	$\frac{l}{\alpha a} \gamma_n N_n \alpha a (\gamma_n N_n \alpha a - 2)$
$I_1 = \int_0^{\alpha a} \int_0^l (X'_m Y'_n)^2 dx ds$	$\frac{(mn)^2 \pi^4}{4l \alpha a}$	$\frac{\gamma_m \gamma_n}{l \alpha a} N_m l N_n \alpha a (\gamma_m N_m l - 2)(\gamma_n N_n \alpha a - 2)$
$I_2 = \int_0^{\alpha a} \int_0^l (X''_m Y_n)^2 dx ds$	$\frac{\alpha a}{4l^3} (m\pi)^4$	$\frac{\alpha a}{l^3} (N_m l)^4$
$I_3 = \int_0^{\alpha a} \int_0^l (X_m Y''_n)^2 dx ds$	$\frac{l}{4(\alpha a)^3} (n\pi)^4$	$\frac{l}{(\alpha a)^3} (N_n \alpha a)^4$
$I_4 = \int_0^{\alpha a} \int_0^l X_m X''_m Y_n^2 dx ds$	$-B_{mn}$	$-B_{mn}$
$I_5 = \int_0^{\alpha a} \int_0^l X_m^2 Y_n Y''_n dx ds$	$-H_{mn}$	$-H_{mn}$
$I_6 = \int_0^{\alpha a} \int_0^l X_m X''_m Y_n Y''_n dx ds$	I_1	I_1

TABLE III. - CALCULATED AND MEASURED FREQUENCIES OF FLAT AND CURVED PANELS

(a) Rectangular panel, 11 inches \times 9 inches \times 0.028 inch (27.94 cm \times 22.86 cm \times 0.071 cm) (ref. 6)

m	Frequencies, cps, for -														
	n = 1			n = 2			n = 3			n = 4			n = 5		
	Simply supported	Experimental	Clamped	Simply supported	Experimental	Clamped	Simply supported	Experimental	Clamped	Simply supported	Experimental	Clamped	Simply supported	Experimental	Clamped
Radius, ∞ (flat)*															
1	56.1	94	103.7	156.9	211	235.5	324.8	394	436.8	560	654	705.75	862.3	957	1042
2	123.5	169	185.3	224.3	286	311.0	392.3	483	509.6	627.4	735	777.8	929.8	1072	1114
3	236.0	297	317.1	336.8	406	436.6	504.7	601	630.0	739.9	845	895.45	1042	1157	1230
4	393.4	472	495.9	494.2	572	611.5	662.1	766	799.95	897.3	998	1061	1200	1317	1394
5	595.8	687	720.35	696.6	790	833.9	864.5	982	1018	1100	1218	1276	1402		1605
Radius, 96 inches (243.84 cm)*															
1	145.7	250	317.1	164.1	233	337.0	325.65	405	483.65	560.1	673	729.4	862.3	999	1055
2	273.7	299	357.95	261.55	351	400.5	399.75	507	553.75	629.3	760	800.9	930.3	1087	1127
3	372.1	532	445.7	392.5	497	511.1	522.3	656	670.4	745.5		917.8	1044	1222	1243
4	498.85	640	589.6	551.2		672.0	686.8	835	836.1	907.3	1068	1083	1204	1389	1407
5	674.6	816	789.5	747.3		882.75	891.6	1052	1050	1113	1302	1296	1408		1618
Radius, 72 inches (182.9 cm)															
1	187.9	269	412.8	169.45	228	398.4	326.3	380	517.1	560.3	618	747.3	862.4	927	1066
2	348.2		448.4	287.2	373	458.15	405.5	491	585.8	630.7	705	818.4	930.8	1012	1137
3	450.3	585	524.4	430.85	516	562.3	535.6	629	700.3	749.9	833	934.7	1046	1127	1253
4	567.5		653.25	591.8	726	715.6	705.3	797	863.2	915.0	988	1099	1207		1417
5	730.1	850	839.4	784.5	905	919.0	912.1		1074	1123	1207	1311	1413		1628
Radius, 48 inches (121.92 cm)															
1	274.8	291	608.2	184.0	289	536.5	328.1	439	602.7	560.6	681	796.2	862.5	988	1094
2	503.8		639.9	350.2	488	592.8	421.4		668.9	634.8		866.4	932.0	1100	1166
3	621.8	622	702.1	525.3	652	687.85	571.9	813	779.2	762.3	979	981.6	1050	1244	1282
4	728.8	778	807.95	694.8	843	827.4	755.8	963	936.25	936.7		1144	1216		1445
5	869.25	943	967.9	882.2		1015	968.3	1152	1140.5	1152		1355	1428	1597	1656

*Experimental values obtained with edges fastened by means of additional clamping frame; all others with simple lap attachment. (See fig. 1.)

TABLE III.- CALCULATED AND MEASURED FREQUENCIES OF FLAT AND CURVED PANELS - Concluded

(b) Rectangular panel, 11 inches \times 9 inches \times 0.048 inch (27.94 cm \times 22.86 cm \times 0.12 cm) (ref. 6 and unpublished experimental data*)

m	Frequencies, cps, for -														
	n = 1			n = 2			n = 3			n = 4			n = 5		
	Simply supported	Experimental	Clamped	Simply supported	Experimental	Clamped	Simply supported	Experimental	Clamped	Simply supported	Experimental	Clamped	Simply supported	Experimental	Clamped
Radius, ∞ (flat)															
1	96.1	182	177.7	268.9	375	403.7	556.8	685	748.8	959.9	1102	1210	1478	1582	1786
2	211.8	314	317.6	384.55	503	533.1	672.5	808	873.7	1076	1228	1333	1594	1734	1910
3	404.5	524	543.6	577.3	693	748.4	865.2	989	1080	1268	1384	1535	1787	1905	2109
4	674.4	787	850.1	847.15	964	1048	1135	1251	1371	1538	1643	1820	2056.5	2134	2389
5	1021	1151	1235	1194	1299	1429.5	1482	1581	1746	1885	1972	2187	2403	2488	2752
Radius, 96 inches (243.84 cm)**															
1	165.3	{ 229 248 }	348.4	273.2	{ 340 366 }	470.2	557.3	{ 632 685 }	777.1	960.0	{ 998 1100 }	1224	1478	{ 1473 1646 }	1794
2	323.2	{ 424 446 }	441.2	407.4	{ 508 531 }	590.0	676.9	{ 770 822 }	900.1	1077	{ ---- 1232 }	1347	1594	{ ---- 1767 }	1917
3	496.4	{ 605 619 }	627.4	611.5	{ 730 754 }	794.2	875.6	{ 968 1015 }	1104	1272	{ 1332 1435 }	1548	1788	{ 1801 1959 }	2117
4	740.9	{ 846 862 }	907.95	881.6	{ 1002 1036 }	1085	1150	{ 1230 1298 }	1393	1544	{ ---- ---- }	1832	2059	{ 2048 ---- }	2397
5	1069	{ 1155 1184 }	1276.5	1224	{ 1322 1368 }	1459	1498	{ 1553 1629 }	1765	1893	{ ---- ---- }	2199	2407	{ ---- ---- }	2759
Radius, 72 inches (182.9 cm)															
1	203.5	233	437.3	276.4	343	516.0	557.7	625	798.4	960.1	993	1235	1478		1800
2	388.4	456	517.3	424.3	513	630.4	680.3	756	920.2	1077.5	1119	1357.5	1594		1923
3	557.4	643	685.5	636.8	731	828.1	883.6	960	1122	1274	1313	1558	1789	1783	2123
4	788.7	884	950.5	907.6	997	1112	1161	1229	1409	1549		1842	2061	2045	2403
5	1105	1197	1308	1247.5	1324	1481	1510	1551	1779	1899		2208	2410		2765
Radius, 48 inches (121.92 cm)															
1	285.6	315	625.1	285.6	400	628.8	558.8	678	856.25	960.3	1040	1265	1478	1521	1817
2	532.3	566	690.0	469.3	597	734.1	689.85	850	975.2	1080	1185	1387	1595	1635	1940
3	703.3	755	829.4	704.1	838	918.0	906.1	1064	1173	1281.5	1400	1587	1791	1864	2139
4	911.7	992	1063	977.85		1187	1192	1339	1455	1561.5		1869	2066	2140	2419.5
5	1202	1294	1394	1311	1441	1542	1545	1677	1820	1916		2234	2418	2460	2781

*Unpublished experimental data obtained from WADC, U.S. Air Force.

**Upper experimental values obtained with edges fastened by means of simple lap attachment, and lower experimental values obtained with edges fastened with an additional clamping frame. (See fig. 1 for edge details.)

TABLE IV.- CALCULATED AND MEASURED FREQUENCIES
OF CURVED PANELS

(a) Rectangular panel, $11\frac{5}{8}$ inches \times $9\frac{5}{8}$ inches \times 0.032 inch
(29.53 cm \times 24.45 cm \times 0.081 cm) (ref. 7)

m	n	Frequencies, cps, for -		
		Theory		Experiment
		Simply supported	Clamped	
a = 96 inches (243.84 cm)				
1	1	146.7	314.4	150
1	2	163.2	334.1	250
1	3	322.8	479.2	440
1	4	554.8	722.5	725
1	5	853.9	1045	
2	1	274.3	356.6	
3	1	373.1	446.4	345
4	1	501.6	593.0	540
5	1	680.1	796.2	800
a = 48 inches (121.92 cm)				
1	1	277.5	602.7	350
1	2	183.2	531.0	270
1	3	323.4	595.05	445*
1	4	551.9	784.7	760
1	5	848.7	1078	
2	1	505.1	635.9	
3	1	622.1	699.9	560
4	1	729.7	808.2	770
5	1	872.3	971.4	935

*Extrapolated from figure 16 of reference 7.

**TABLE IV.- CALCULATED AND MEASURED FREQUENCIES
OF CURVED PANELS – Concluded**

(b) Square panels; 17.0 inches \times 17.0 inches (43.18 cm \times 43.18 cm)*;
various thickness; m = 1 (ref. 8)

n	Frequencies, cps, for –					
	a = 96 inches (243.84 cm)			a = 48 inches (121.92 cm)		
	Theory		Experiment	Theory		Experiment
	Simply supported	Clamped		Simply supported	Clamped	
h = 0.020 inch (0.051 cm)						
1	167.3	299.5	240	332.7	597.3	310
2	74.6	245.9		137.4	484.1	
3	74.4	225.55	85	94.1	423.7	86
4	114.7	232.3	129	119.55	393.7	148
5	173.3	267.1	190	174.7	392.9	241
6	246.2	326.9		246.6	421.1	387
7	332.5	407.7	345	332.6	476.9	439
h = 0.032 inch (0.081 cm)						
1	168.1	301.0		333.1	598.1	
2	85.3	253.6	117	143.5	488.0	102
3	111.5	251.6	125	125.4	438.1	144
4	181.9	292.6	229	184.9	432.0	270
5	276.9	373.4	295	277.6	471.6	294
6	393.7	486.7		393.9	554.3	
7	532.0	627.4		532.0	674.4	613
h = 0.040 inch (0.010 cm)						
1	168.9	302.4		333.5	598.8	
2	94.2	260.5	123	148.9	491.65	169
3	137.1	273.4	197	148.6	451.0	180
4	226.9	338.8	278	229.2	464.5	289
5	346.0	449.7	388	346.5	534.0	398
6	492.1	597.4		492.2	653.6	
7	665.0	776.9	727	664.9	815.2	735

*Actual unsupported length between opposite edges of support frame.

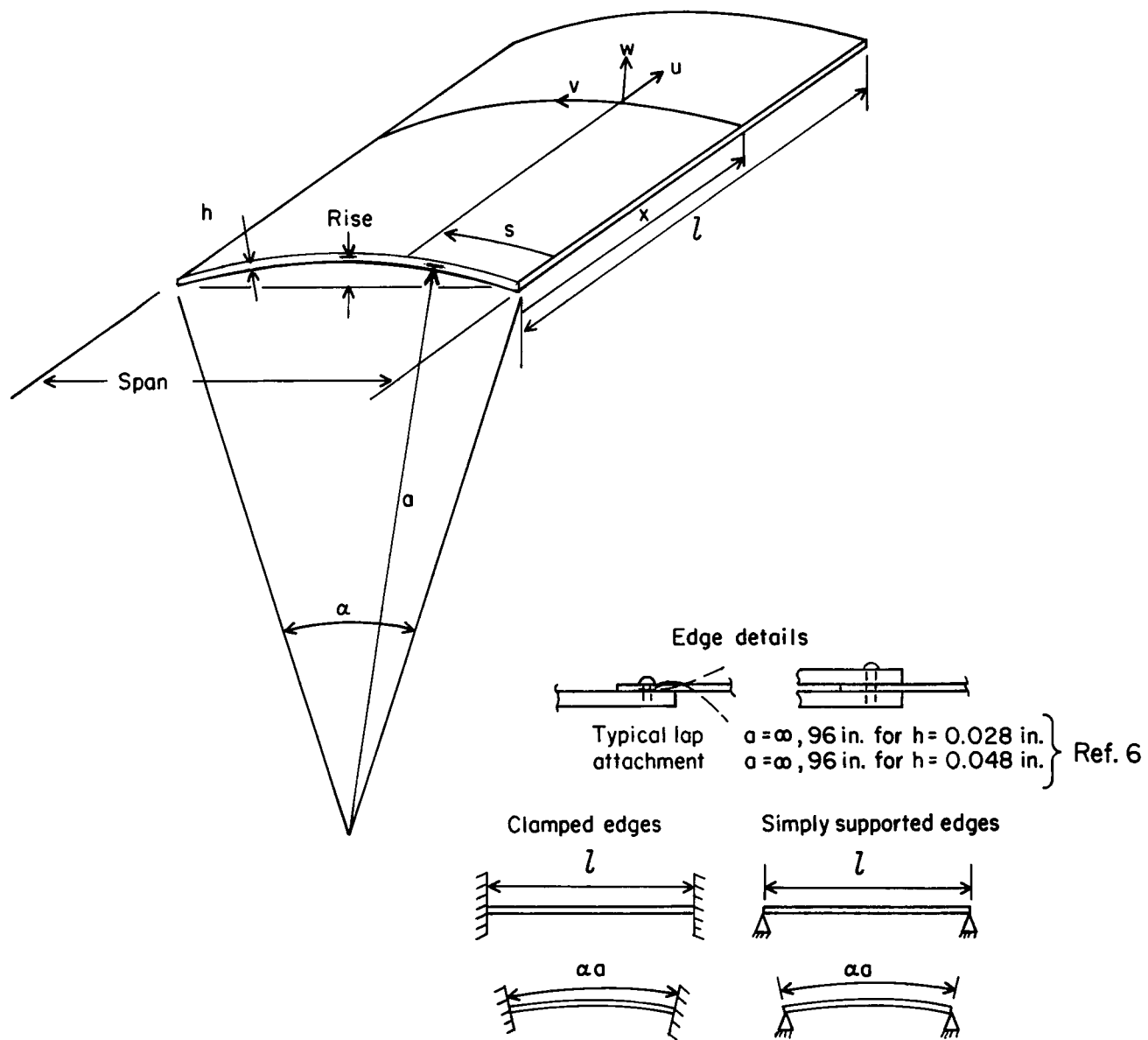


Figure 1.- Analytical vibration model of cylindrically curved panel.

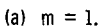
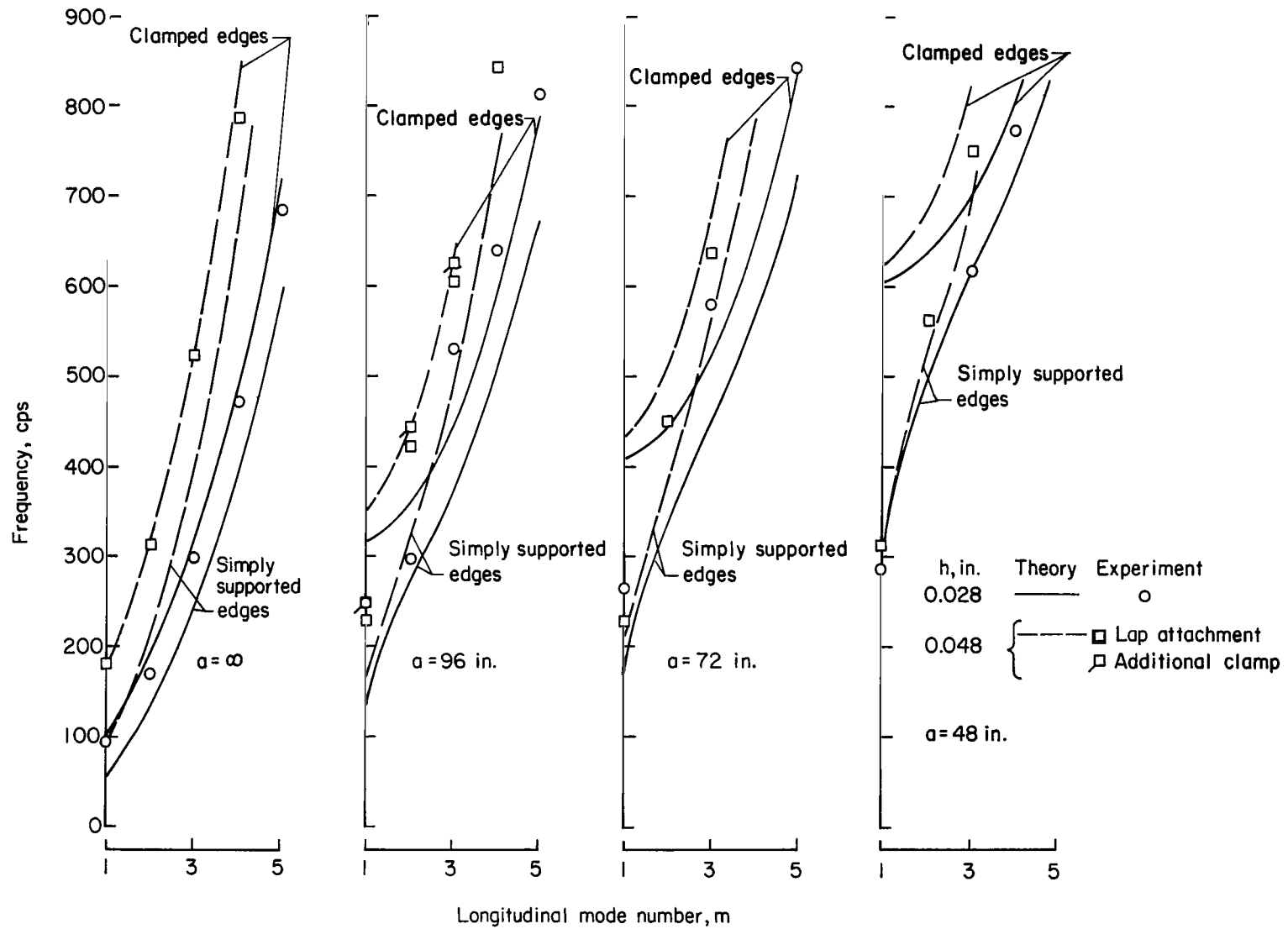
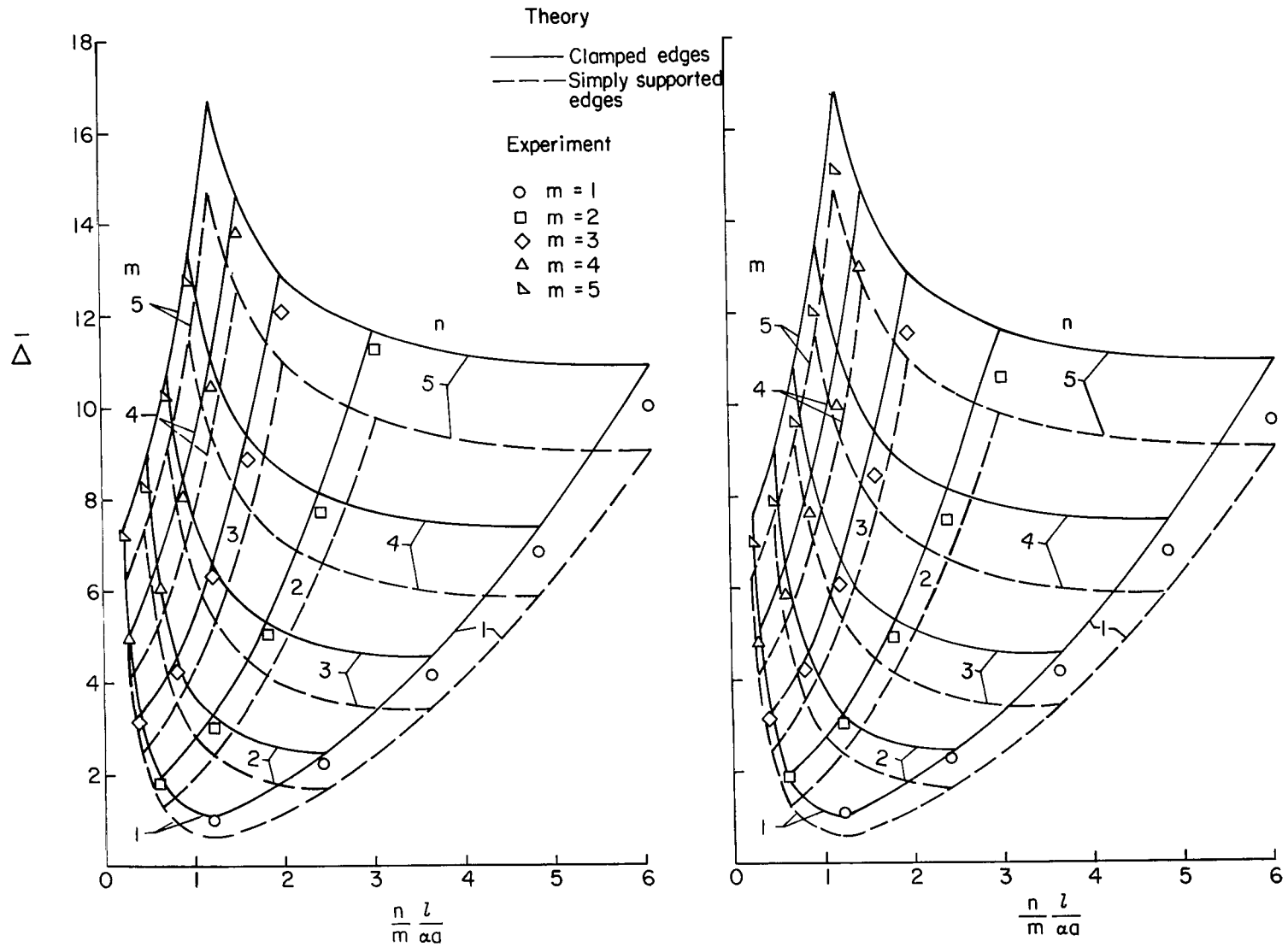


Figure 2.- Comparison of calculated and measured natural frequencies of flat and curved rectangular aluminum panels of two thicknesses (ref. 6). Additional clamp for $h = 0.028$ inch (0.07 cm), $a = \infty$, 96 inches (243.84 cm); lap attachment for all others except as noted.



(b) $n = 1$.

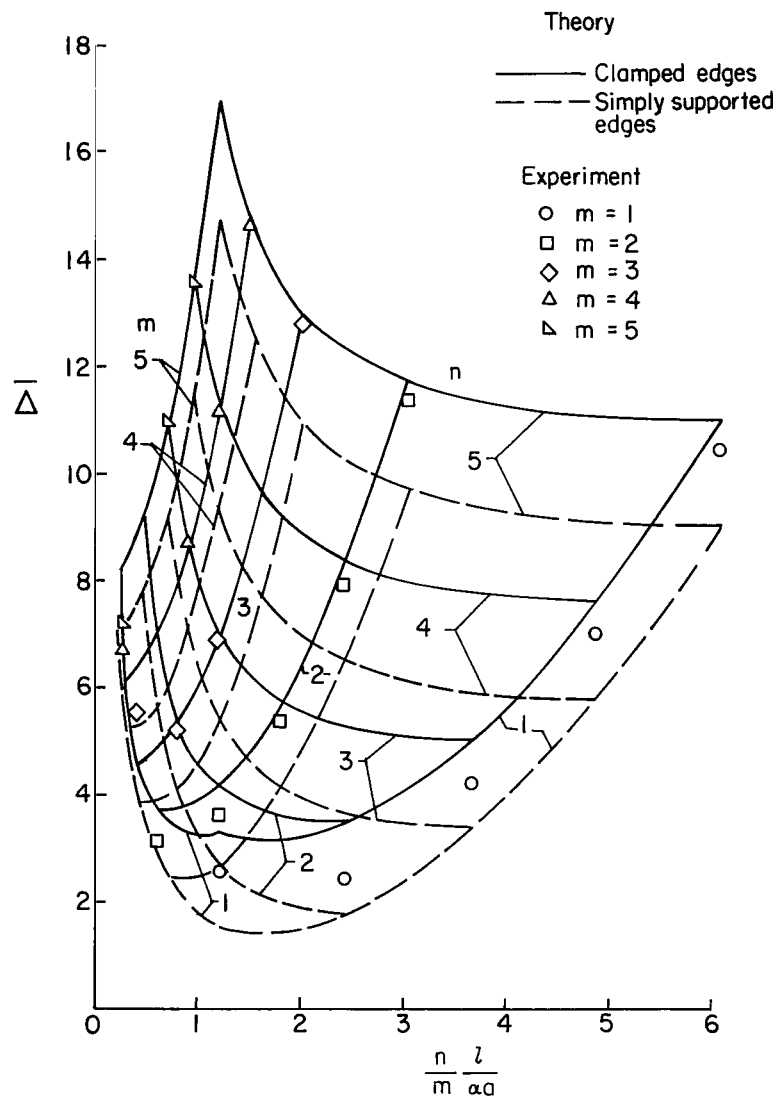
Figure 2.- Concluded.



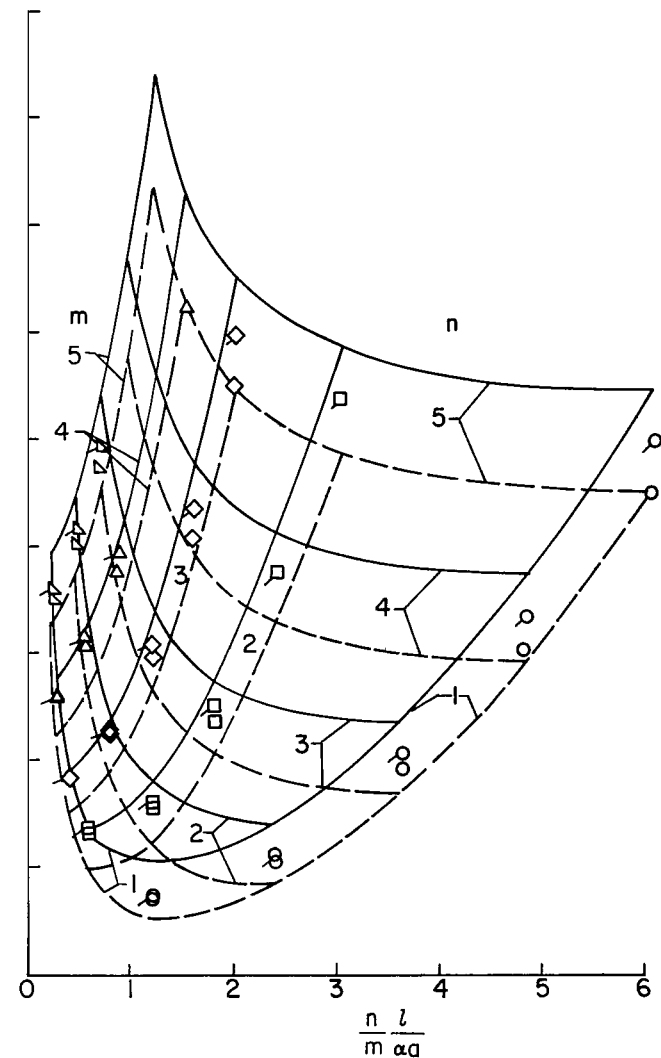
(a) $a = \infty$ (flat panel). $h = 0.028$ inch (0.07 cm); experimental edge support; additional clamp frame.

(b) $a = \infty$ (flat panel). $h = 0.048$ (0.12 cm); experimental edge support; simple lap attachment.

Figure 3.- Comparison of calculated and measured dimensionless frequency parameters for rectangular aluminum panels (ref. 6).

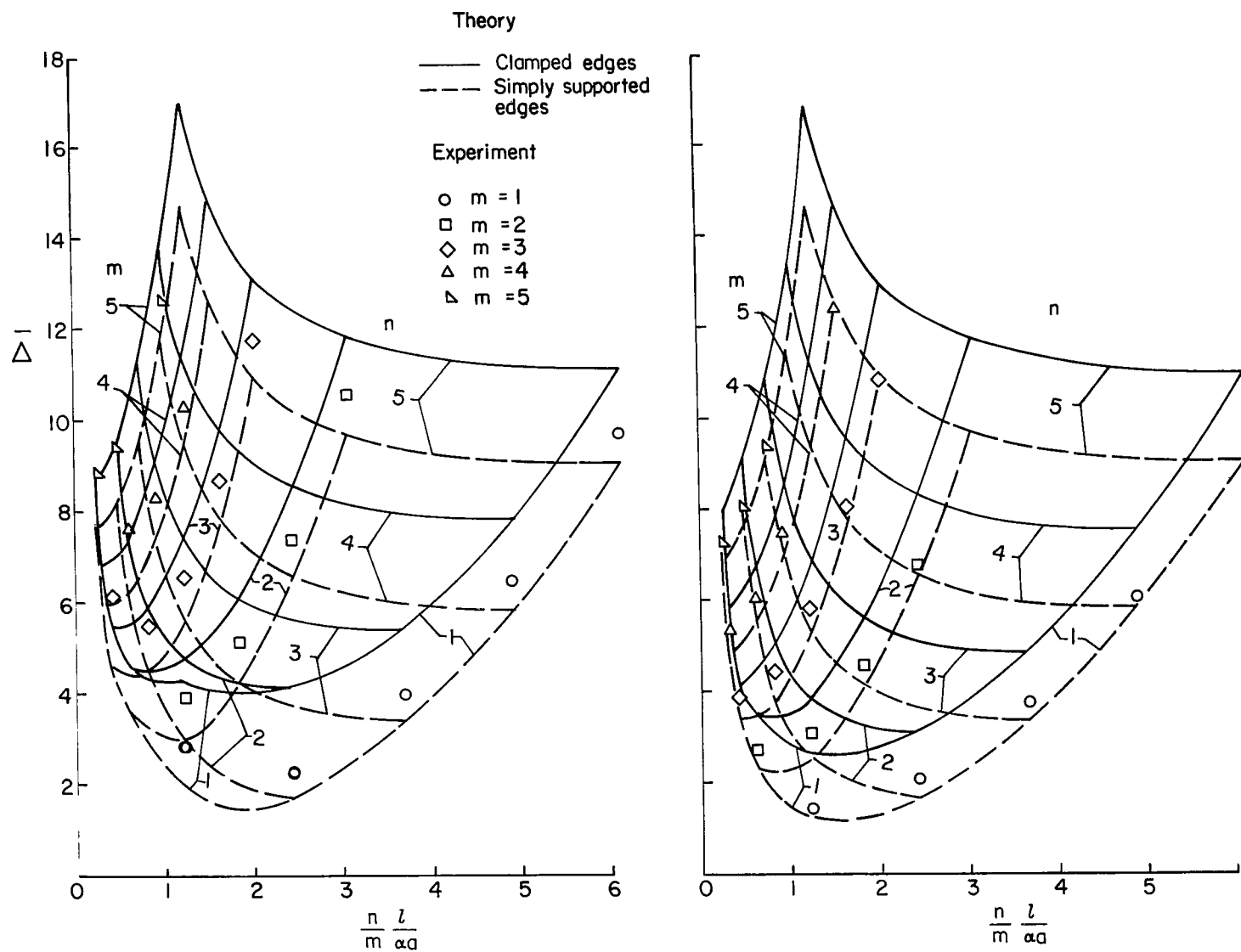


(c) $a = 96$ inches (243.84 cm). $h = 0.028$ inch (0.07 cm); additional clamped frame.



(d) $a = 96$ inches (243.84 cm). $h = 0.048$ inch (0.12 cm); additional clamped frame (flagged symbols); simple lap attachment (plain symbols).

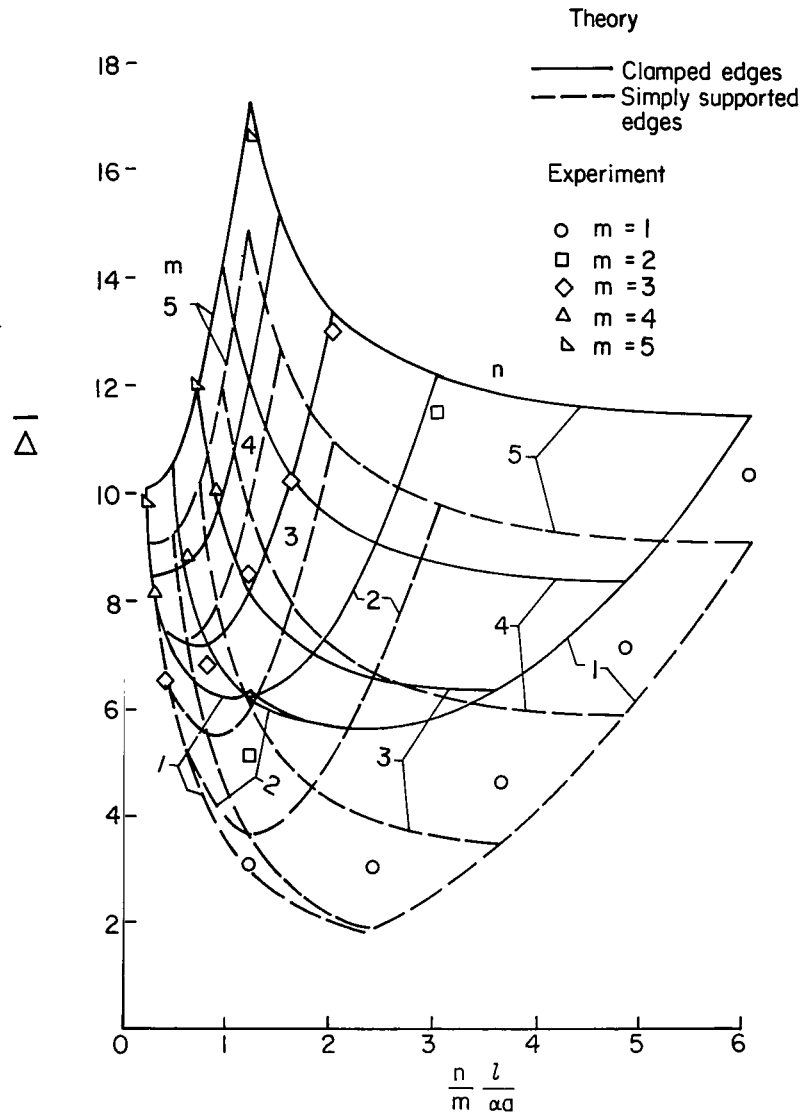
Figure 3.- Continued.



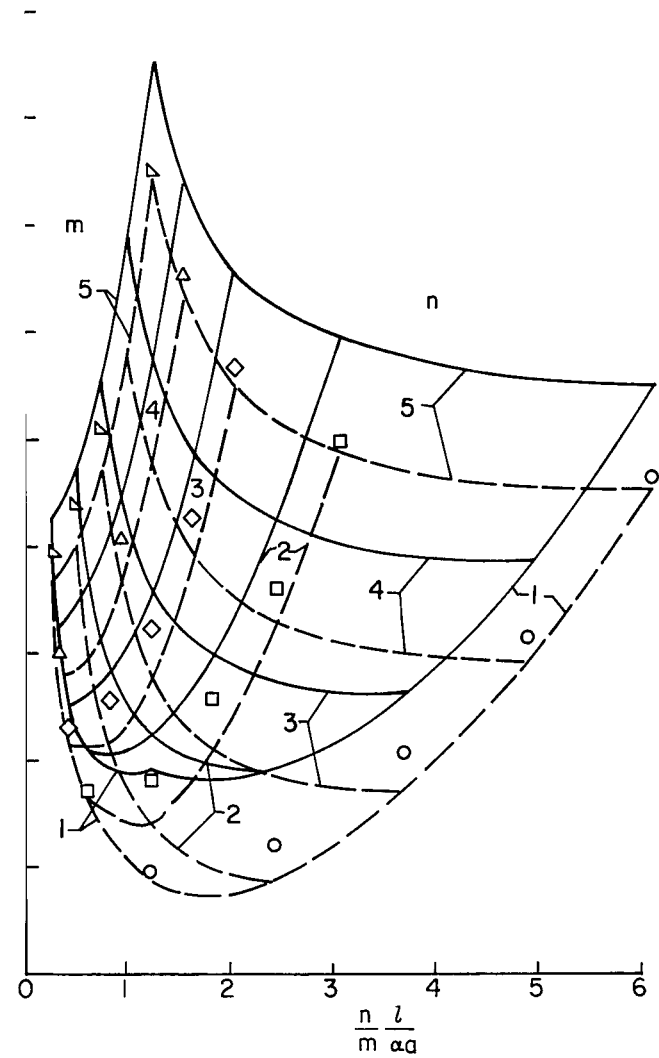
(e) $a = 72$ inches (177.88 cm), $h = 0.028$ inch (0.07 cm); simple lap attachment.

(f) $a = 72$ inches (177.88 cm), $h = 0.048$ inch (0.12 cm); simple lap attachment.

Figure 3.- Continued.



(g) $a = 48$ inches (121.92 cm). $h = 0.028$ inch (0.07 cm); simple lap attachment.



(h) $a = 48$ inches (121.92 cm). $h = 0.048$ inch (0.12 cm); simple lap attachment.

Figure 3.- Concluded.

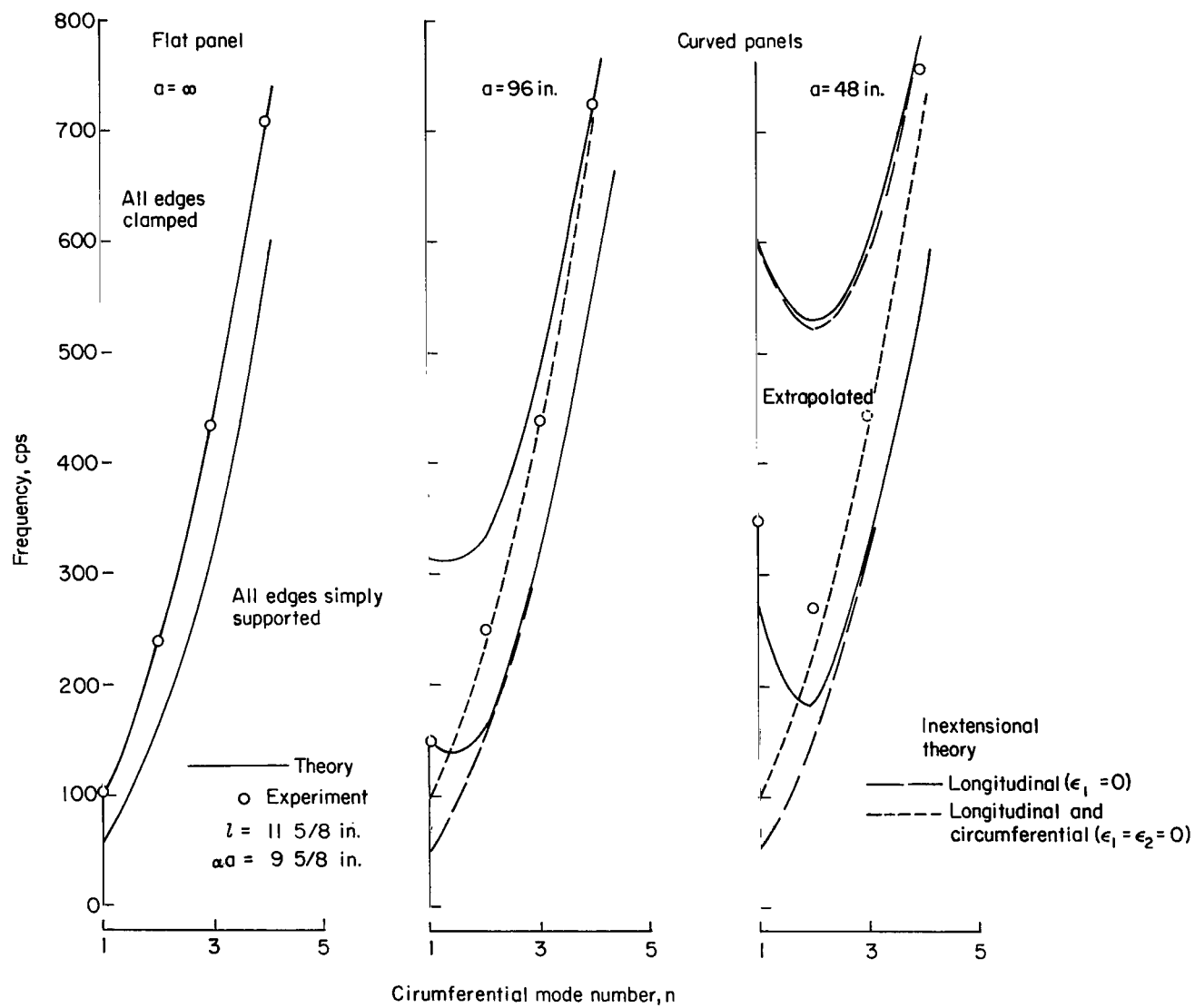
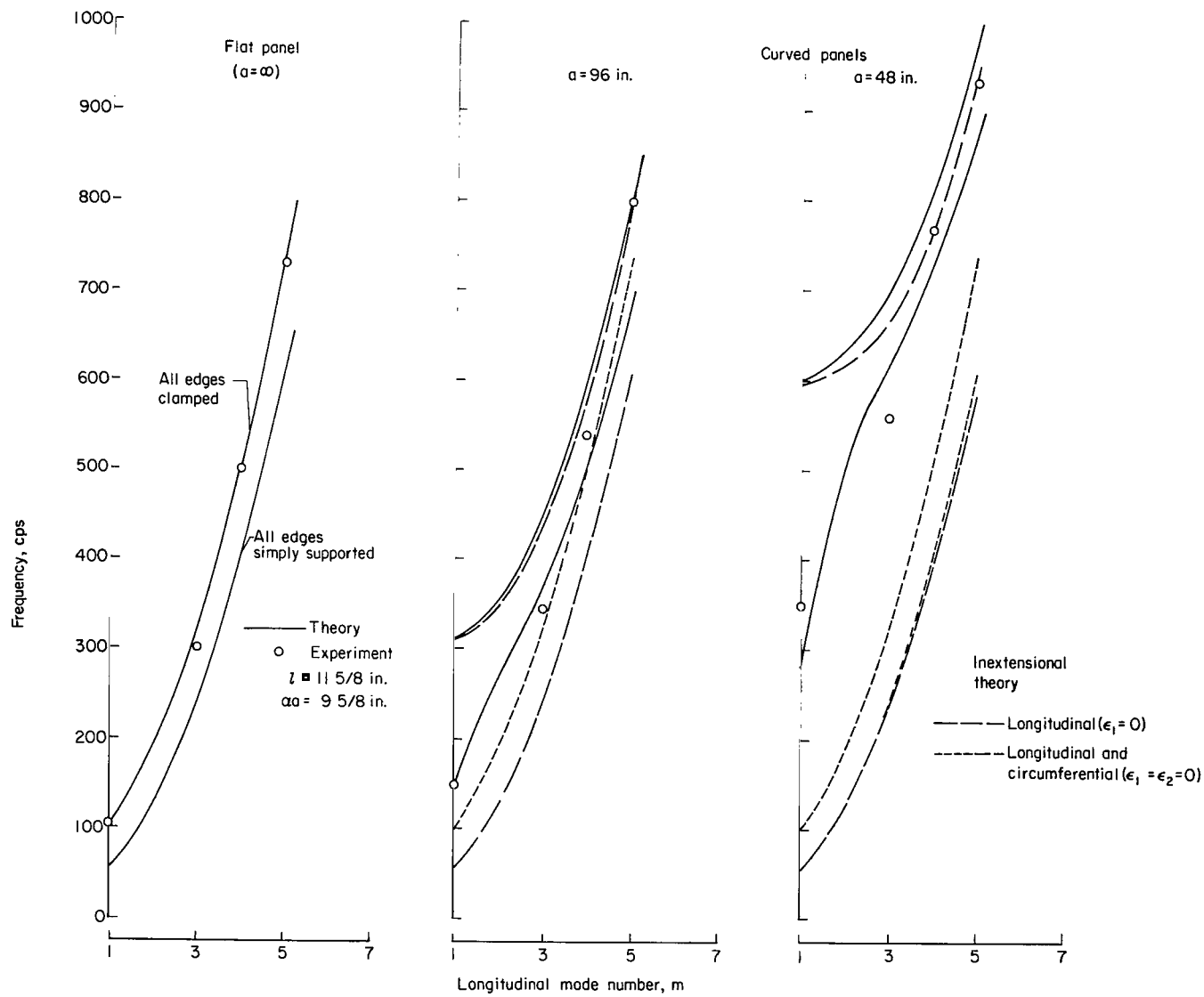
(a) $m = 1$.

Figure 4.- Comparison of calculated and measured natural frequencies of flat and curved 0.032-inch-thick rectangular aluminum panels (ref. 7).



(b) $n = 1$.

Figure 4.- Concluded.

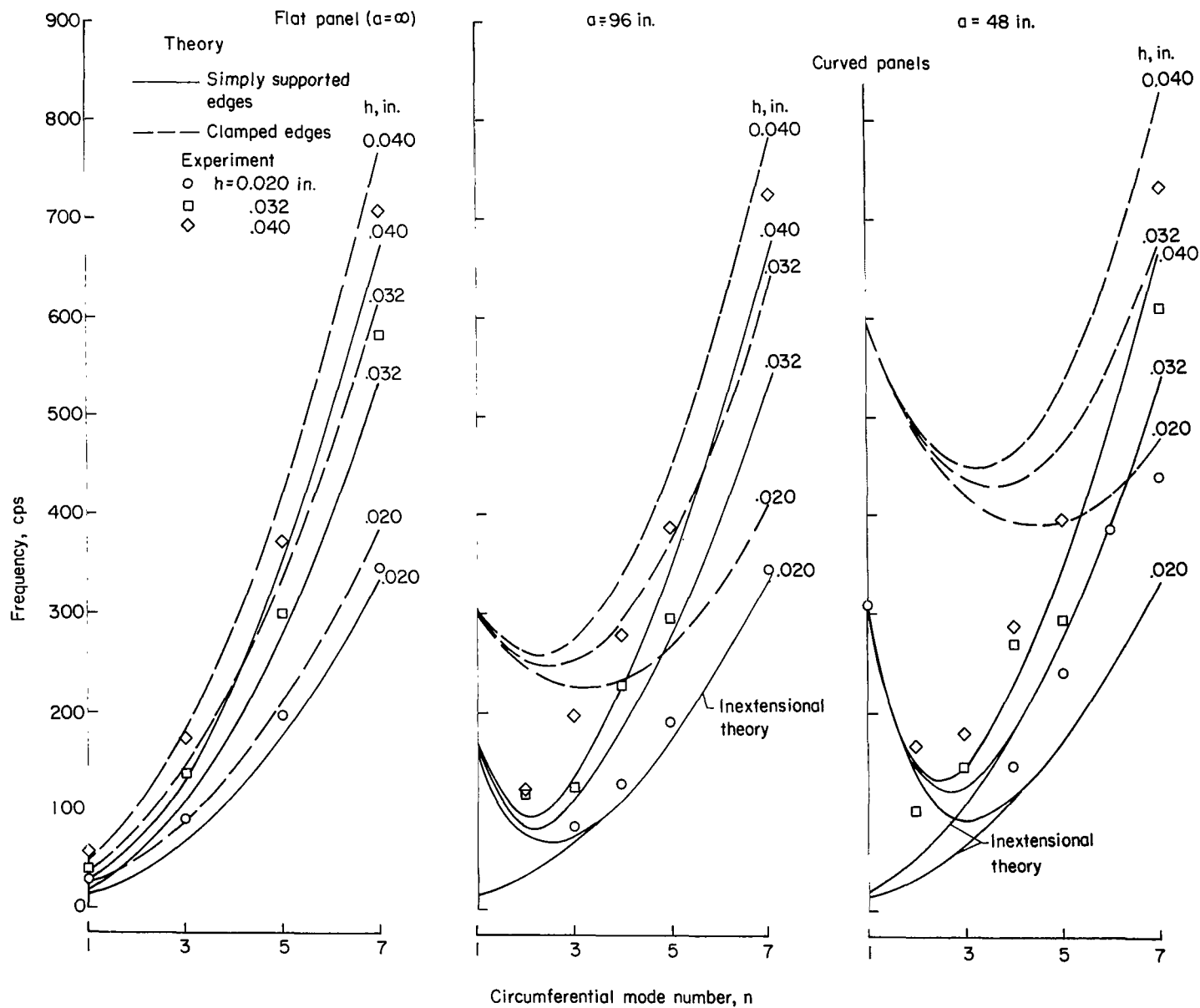


Figure 5.- Comparison of calculated and measured natural frequencies of flat and curved 17-inch-square aluminum panels (ref. 8); $m = 1$.

"The aeronautical and space activities of the United States shall be conducted so as to contribute . . . to the expansion of human knowledge of phenomena in the atmosphere and space. The Administration shall provide for the widest practicable and appropriate dissemination of information concerning its activities and the results thereof."

—NATIONAL AERONAUTICS AND SPACE ACT OF 1958

NASA SCIENTIFIC AND TECHNICAL PUBLICATIONS

TECHNICAL REPORTS: Scientific and technical information considered important, complete, and a lasting contribution to existing knowledge.

TECHNICAL NOTES: Information less broad in scope but nevertheless of importance as a contribution to existing knowledge.

TECHNICAL MEMORANDUMS: Information receiving limited distribution because of preliminary data, security classification, or other reasons.

CONTRACTOR REPORTS: Technical information generated in connection with a NASA contract or grant and released under NASA auspices.

TECHNICAL TRANSLATIONS: Information published in a foreign language considered to merit NASA distribution in English.

TECHNICAL REPRINTS: Information derived from NASA activities and initially published in the form of journal articles.

SPECIAL PUBLICATIONS: Information derived from or of value to NASA activities but not necessarily reporting the results of individual NASA-programmed scientific efforts. Publications include conference proceedings, monographs, data compilations, handbooks, sourcebooks, and special bibliographies.

Details on the availability of these publications may be obtained from:

SCIENTIFIC AND TECHNICAL INFORMATION DIVISION
NATIONAL AERONAUTICS AND SPACE ADMINISTRATION

Washington, D.C. 20546